CRACK DETECTION IN BEAMS THROUGH MULTI-TONE HARMONIC EXCITATION

by
SHARAD DWIVEDI

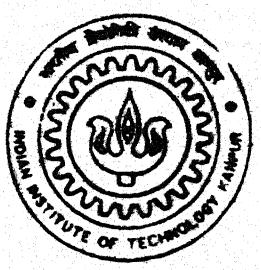

DEPARTMENT OF MECHANICAL ENGINEERING
INDIAN INSTITUTE OF TECHNOLOGY KANPUR

February, 2000

CRACK DETECTION IN BEAMS THROUGH MULTI-TONE HARMONIC EXCITATION

A Thesis Submitted
in Partial Fulfillment of the Requirements
for the Degree of

MASTER OF TECHNOLOGY

February, 2000

by

SHARAD DWIVEDI

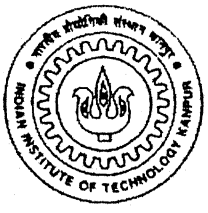

DEPARTMENT OF MECHANICAL ENGINEERING
INDIAN INSTITUTE OF TECHNOLOGY
KANPUR – 208016 (INDIA)

CERTIFICATE

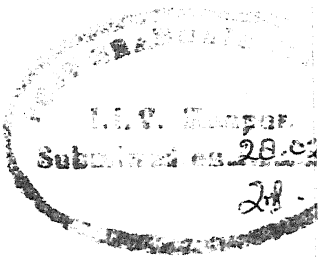

It is certified that the work contained in the thesis entitled, "CRACK DETECTION IN BEAMS THROUGH MULTI-TONE HARMONIC EXCITATION" by *Mr. Sharad Dwivedi* has been carried out under my supervision and that this work has not been submitted elsewhere for a degree.

Nalinaksh Vyas. 28.2.2000

Dr. N.S.Vyas
(Professor)
Department of Mechanical Engineering,
Indian Institute of Technology, Kanpur.

February, 2000

ACKNOWLEDGEMENTS

I wish to put on record the enormous debt of gratitude I owe to my guide Prof. Vyas for his inspiring guidance, invaluable suggestions and constructive criticism. He was always a constant source of encouragement throughout my thesis work. The kind of helpfulness shown by him is simply rare. I am also thankful to Dr. Raghuram for his timely help.

I am thankful to Mr Animesh Chatterjee and Ms. Lalitha who helped me throughout my thesis work. I heartily appreciate the keen interest shown by Amod, Sunil and Nivea in successful completion of my thesis work. I appreciate the help provided by Mr. M.M.Singh and Mr. Verma for conducting the experiments.

A number of persons have contributed, either directly or indirectly towards completion of this work. I am grateful to all of them.

Finally, I would like to thank all my friends for making my stay at IITK a memorable one.

Indian Institute Of Technology, Kanpur. Sharad Dwivedi

Feb' 2000.

ABSTRACT

The present study attempts to explore the possibility of crack detection in beams, through multi-tone harmonic excitation and higher order FRF analysis. A transverse crack in a beam has been modeled as a bilinear single degree freedom system, exhibiting breathing characteristics. A breathing crack opens or closes depending on the direction of the vibration. The response of such a system is examined under single tone, two tone and three tone excitations. The difference between the excitation frequencies is kept such that their harmonics occur at the natural frequency of the system, so as to magnify small amounts of bilinearity, which could have developed in a system originally taken as linear. Development of an equivalent polynomial nonlinear form to represent bilinear stiffness, is suggested for better understanding of the response harmonics. A step-by-step procedure for crack detection is developed. Numerical simulation is carried out through MATLAB toolbox to illustrate the procedure. Experimental work carried out on a laboratory beam set-up is also reported.

CONTENTS

LIST OF FIGURES

CHAPTER 1

INTRODUCTION

Damage detection by means of non-destructive testing plays an important role in ensuring the integrity of machine elements and structures. Vibration testing is an effective means of detecting crack development in structures. Fatigue cracks often exist in structural members that are subjected to repeated loading. Various studies have been carried out on the dynamic response of fatigue cracks, in an attempt to find viable vibration testing procedures for health monitoring. The crack models used in these analyses fall largely into two categories:(1) open crack models and (2) opening and closing or breathing crack models.

1.1 Open Crack Model

A beam is made more compliant by an open crack. The consequent reductions in the natural frequencies of free vibrations and changes in mode shapes have motivated a number of researchers to seek simple means for identifying and characterizing cracks in structures. Cawley and Adams (1979) developed an experimental technique to identify the cracks from changes in natural frequencies. Gudmunson (1982) used a first order perturbation method to predict the change in resonance frequencies of a structure due to cracks, notches or other geometrical changes. Christides and Barr (1984) examined the special case of symmetric double sided crack. They used variational principles to formulate a fourth order partial differential equation for a Bernoulli-Euler beam with a double sided crack. Mathematically and experimentally, they found that the drop in the first natural frequency was very small unless the crack was fairly large. Gounaris and Dinarogonas (1988) modelled a crack with an equivalent rotational spring constant, calculated via an application of Castigliano's theorem. They also found that the changes in the natural frequencies were significant only for large cracks. Rizos et al (1989) conducted experiments to detect crack depth and location from changes in the mode shapes of cantilever beams. They forced a cracked beam with known crack characteristic in resonance and measured vibration amplitude at two arbitrarily chosen position on the beam. Further research on crack identification via natural frequency changes was done by Anifantis et al. They found that

he size and position of large cracks can be found if the change in the first two natural requencies were known for a simply-supported Bernoulli-Euler beam. Rajab and Al-Sabeeh 1991) found that knowledge of the changes in the first three natural frequencies of a Timoshanko beam was sufficient to determine the size and locations of large cracks. Gounaris et al (1991) modelled cracked hollow beams with the finite element method , but encountered a sensitivity problem with small cracks. Ostachowicz and Krawczuk (1991) examined the effect of more than one crack on the natural frequencies of a cantilever beam, yielding comparable results. Reference can also be made to the studies by Pandey et al (1991), Nandwana and Maiti (1997), Tsai and Wang (1996),on analysis of open crack models.

1.2 Breathing Crack Model

Open crack models, however are inadequate in correctly representing the phenomenon due to the assumption that the cracks are always open in vibration. A breathing crack model is a more realistic representation. The basic concept is that the crack alternatively opens and closes depending on the direction of vibration. When the crack is closed, the beam acts approximately, as a homogeneous beam with no crack, while when the crack is open, a local reduction of flexural rigidity occurs. Recently, increasing efforts have focussed on vibration analysis using opening and closing models to simulate a fatigue crack. A single-degree-of-freedom, non-linear model was proposed by Friswell and Penny (1992). A mathematical model of a beam, with a closing crack was developed by Krawczuk and Ostachowicz (1994), who examined the possibility of crack detection on the basis of changes of the high harmonics in the frequency spectrum. Abraham and Brandon (1995) presented a substructure model to predict the vibration properties of a beam with a breathing transverse crack. Dimarogonas and Papadopoulos (1983) have obtained analytical solutions for the closing crack, for rotating shafts, under the assumption of large static deflection. Gudmunson (1983) pointed out that the alteration in natural frequencies due to a real fatigue crack is much lower than the drop caused by the narrow notch. Ibrahim et al (1987) confirmed the result and employed a bond-graph model to simulate the dynamic behavior of a cantilever beam including a non-linear fatigue crack. Qian et al (1990) observed that the difference of the amplitude response between the integral and cracked beam is reduced if a closing crack model is considered. The salient features of the studies cited above can be summarized as -

) Natural frequency reduction for a fatigue crack (breathing crack) is much smaller than for an open crack and that fatigue cracks would be difficult to recognize by frequency monitoring. Also, crack detection by an open crack model would underestimate the crack severity if the crack was actually growing under fatigue loading conditions.

ii) The experimental studies reveal the presence of super/sub-harmonic vibration phenomena.

iii) Detection of fatigue cracks should be more reliably based on non-linear features of FRF, rather than the natural frequency shift.

1.3 Present Study

The focus of the present study is to analyze the bilinear model of a cracked beam. The bilinear model is discussed in the next chapter. The proposed crack detection procedure involves multi-tone harmonic excitation. Numerical simulation of the response is discussed in Chapter 3. An equivalent polynomial form of nonlinear modeling is done and the response is represented as a Volterra series, in order to rationalize the numerical results. Experimental investigations are described in Chapter 4. Chapter 5 gives the conclusions and scope for further investigations.

CHAPTER 2

NONLINEAR MODELS OF A CRACKED BEAM

Nonlinear models of a cracked beam are discussed in this chapter. Damping is assumed to be linear and only stiffness nonlinearity is considered. Two forms of nonlinear spring force representation are considered – (i) Bilinear function and (ii) Polynomial function.

Bilinear oscillators, due to their simplicity, appear to be appropriate to simulate the behaviour of fatigue cracks in structures. The fundamental assumption is that the beam vibrates mainly in its first mode. The exactness of this assumption depends on the position and the kind of force exciting the structure. A transverse crack, as shown in Fig. 2.1, will alternately open and close under the action of an excitation force. When the crack is in the compression (closed) the equivalent stiffness may be regarded as that of a beam without a crack, due to the contact of the crack walls. On the other hand, when the crack is in tension (crack open) the beam stiffness will reduce near the crack. The equivalent stiffness, of this model, therefore takes two different values depending on whether or not the crack is open. The equivalent damping of the beam is assumed to be constant although the system has increasing damping due to the friction forces at the point of the crack closure. Such a model was considered by Shen and Chu (1992), by deriving a bilinear equation of motion for each vibration mode of a simply supported beam. However, an analytical representation of the response of a bilinear system is approximate. Galerkin procedure was employed by Shen and Chu to simulate the response. Rivola and White (1998) idealized the cracked beam as a simple SDOF system with bilinear stiffness characteristics. They presented a procedure to obtain approximate analytical expressions of the response of bilinear oscillators. This procedure is briefly outlined below.

2.1 The Bilinear Model

The simple bilinear single-degree-of-freedom bilinear model of a cracked beam, shown in Fig.2.2, can be described by (Rivola and White, 1998)

$$m\ddot{u} + c\dot{u} + \tilde{k}(u)u = f(t) \tag{2.1}$$

where $u(t)$ is the displacement of the oscillator, m is the mass, c the damping coefficient and $\tilde{k}(u)$ is a piecewise stiffness function defined as

$$\tilde{k}(u) = \{k, if\ u < 0$$
$$k\alpha\ if\ u > 0\ \} \qquad \text{with } 0 \le \alpha \le 1 \tag{2.2}$$

The relationship between the restoring force and the displacement of the bilinear system is depicted in Fig.2.3. For free undamped vibration of the oscillator, the period of the system is composed of two half sinewaves, and a bilinear radian frequency ω_0, is defined as (Choi and Noah, 1988)

$$\omega_0 = 2\omega_1\omega_2 /(\omega_1 + \omega_2) \tag{2.3}$$

where

$$\omega_1 = \sqrt{k/m} \qquad \omega_2 = \sqrt{\alpha k/m} \tag{2.4}$$

Obtaining a closed form solution of equation (2.4) is quite difficult. Kraczuk and Ostachowicz (1994) found the solution for a harmonic excitation force, by approximating the stiffness force through a square-wave function $s(t)$, having a frequency equal to the forcing frequency as follows

$$m\ddot{u} + c\dot{u} + k[1-(1-\alpha)s(t)]u = f(t) \tag{2.5}$$

The square-wave function $s(t)$, given in Fig. 2.4, changes between 0 and 1, and can be approximated by the complex Fourier series

$$s(t) = \sum_{n=-\infty}^{\infty} q_n e^{in\omega t}, \tag{2.6}$$

where ω is the excitation frequency and q_n are Fourier coefficients

$$q_n = \frac{(-1)}{n\pi}\cos[\frac{\pi}{2}(n+1)] \text{ if } n \neq 0, \quad q_n = 1/2 \quad \text{if } n = 0 \tag{2.7}$$

Using equations (2.6) and (2.7) in (2.5), the equation of motion becomes

$$m\ddot{u} + c\dot{u} + k[1-(1-\alpha)\sum_{-\infty}^{\infty} q_n e^{in\omega t}]u = \frac{f_0}{2}e^{-i\omega t} + \frac{f_0}{2}e^{i\omega t} \tag{2.8}$$

It is to be noted that the above equation represents only an approximation of the spring force variation. Rivola and White (1998) further employed the harmonic balance method to transform the above equation into a set of linear equations, which were then solved numerically.

2.2 The Polynomial Model

While, representation of a cracked beam through a bilinear spring model helps in understanding the role of the opening and closing of crack, on the spring forces developed by the beam over a cycle of vibration, the absence of an analytical solution restricts its utility in understanding the response phenomenon. In this context, an interesting study reported by Sundermeyer and Weaver (1995) can be discussed. They carried out a numerical simulation on a bilinear oscillator. It was excited by two sinusoidal forces with different forcing frequencies. They observed that if the difference of the two forcing frequencies is approximately equal to the fundamental frequency of the system, in addition to the peaks at the two forcing frequencies, a peak is also observed at the natural frequency, in the FRF of the response of the cracked beam. This has been graphically described in Fig.2.5. Sundermeyer and Weaver, while pointing at the possibility of employing, the occurrence of this additional peak at the natural frequency, as a tool to detect the presence of a crack, do not provide analytical reasons for this behaviour of a beam with crack.

Analysis of the above behaviour can be attempted through a polynomial representation of the cracked beam stiffness. The emphasis of the present study is to investigate the response pattern of the bilinear oscillator through its better analytical representation, which can help in modifying and refining the crack detection procedure suggested by Sundermeyer and Weaver.

The nonlinear spring force described by the bilinear oscillator, representing a cracked beam can be approximated through a polynomial function as illustrated in Fig. 2.6 and given by

$$g(x) = k_1 x + k_2 x^2 + k_3 x^3 + k_4 x^4 + k_5 x^5 \tag{2.9}$$

This polynomial function approximation renders the governing equation (2.1 and 2.2), as

$$m\ddot{x} + c\dot{x} + k_1 x + k_2 x^2 + k_3 x^3 + k_4 x^4 + k_5 x^5 = f(t) \tag{2.10}$$

Using Volterra series representation (Schetzen, 1980) of the response, $x(t)$ is expressed as

$$x(t) = \sum_{n=1}^{\infty} x_n(t) \tag{2.11}$$

with the nth order response component being given by

$$x_n(t) = \int_{-\infty}^{\infty}\int_{-\infty}^{\infty}\cdots\int_{-\infty}^{\infty} h_n(\tau_1,\tau_2,...,\tau_n) f(t-\tau_1) f(t-\tau_2)...f(t-\tau_n) d\tau_1 d\tau_2 ... d\tau_n \tag{2.12}$$

$h_n(\tau_1,\tau_2,...,\tau_n)$ is nth order Volterra kernel and its Fourier transform provides the nth order Frequency Response Function (Schetzen, 1980) as

$$H_n(\omega_1,\omega_2,...,\omega_n) = \int_{-\infty}^{\infty}\int_{-\infty}^{\infty}\cdots\int_{-\infty}^{\infty} h_n(\tau_1,\tau_2,...,\tau_n)\prod_{i=1}^{n} e^{-j\omega_i\tau_i} d\tau_1 d\tau_2 ... d\tau_n \tag{2.13}$$

Employing the above, the individual response components (equation 2.12), can be expressed, after some algebra as

$$x_n(t) = (A/2)^n \sum_{p+q=n} {}^nC_q \, H_n^{p,q}(\omega) e^{j\omega_{p,q} t} \qquad 0 \le p \le n; \quad 0 \le q \le n \tag{2.14}$$

where the following brief notations have been used

$$H_n^{p,q}(\omega) = H_n(\underbrace{\omega,.....,\omega}_{p\ times},\underbrace{-\omega,.....,-\omega}_{q\ times}) \qquad \omega_{p,q} = (p-q)\omega \tag{2.15}$$

2.2.1 Response to Single-Tone-Excitation

Restricting the spring force nonlinearity, in equation (2.10), upto the cubic term only and a single tone harmonic excitation

$$f(t) = A\cos\omega t = \frac{A}{2}e^{j\omega t} + \frac{A}{2}e^{-j\omega t} \tag{2.16}$$

the Volterra series response becomes

$$x(t) = x_1(t) + x_2(t) + x_3(t) + ... \tag{2.17}$$

where the individual response components $x_1(t), x_2(t), x_3(t)$ are

$$\begin{aligned} x_1(t) &= \int_{-\alpha}^{\alpha} h_1(\tau)\left[\frac{A}{2}e^{j\omega(t-\tau)} + \frac{A}{2}e^{-j\omega(t-\tau)}\right] d\tau \\ &= \int_{-\alpha}^{\alpha}\left[\frac{A}{2}e^{j\omega t}h_1(\tau)e^{-j\omega t} + \frac{A}{2}e^{-j\omega t}h_1(\tau)e^{j\omega t}\right] d\tau \\ &= \frac{A}{2}e^{j\omega t}\int_{-\alpha}^{\alpha} h_1(\tau)e^{-j\omega t} d\tau + \frac{A}{2}e^{-j\omega t}\int_{-\alpha}^{\alpha} h_1(\tau)e^{j\omega t} d\tau \\ &= \frac{A}{2}e^{j\omega t}H_1(\omega) + \frac{A}{2}e^{-j\omega t}H_1(-\omega) \\ &= \frac{A}{2}H_1(\omega)e^{j\omega t} + \frac{A}{2}H_1(-\omega)e^{-j\omega t} \end{aligned} \tag{2.18}$$

$$
\begin{aligned}
x_2(t) &= \int_{-\infty}^{\infty}\int_{-\infty}^{\infty} h_2(\tau_1,\tau_2)\left[\frac{A}{2}e^{j\omega(t-\tau_1)}+\frac{A}{2}e^{-j\omega(t-\tau_1)}\right]*\left[\frac{A}{2}e^{j\omega(t-\tau_2)}+\frac{A}{2}e^{-j\omega(t-\tau_2)}\right]d\tau_1 d\tau_2 \\
&= \int_{-\alpha}^{\alpha}\int_{-\infty}^{\infty} h_2(\tau_1,\tau_2)\left[\frac{A}{4}e^{j\omega(2t-\tau_1-\tau_2)}\frac{A^2}{4}e^{-j\omega\tau_1+j\omega\tau_2}+\frac{A^2}{4}e^{j\omega\tau_1-j\omega\tau_2}+\frac{A^2}{4}e^{-2j\omega t+j\omega\tau_1+j\omega\tau_2}\right]d\tau_1 d\tau_2 \\
&= \frac{A^2}{4}e^{j2\omega t}\int_{-\infty}^{\infty}\int_{-\alpha}^{\alpha} h_2(t_1,\tau_2)e^{-j\omega\tau_1-j\omega\tau_2}d\tau_1 d\tau_2+\frac{A^2}{4}\int_{-\alpha}^{\alpha}\int h_2(t_1,\tau_2)e^{-j\omega\tau_1+j\omega\tau_2}d\tau_1 d\tau_2 \\
&+\frac{A^2}{4}\int_{-\alpha}^{\alpha}\int h_2(t_1,\tau_2)e^{j\omega\tau_1-j\omega\tau_2}d\tau_1 d\tau_2+\frac{A^2}{4}e^{-2j\omega t}\int_{-\alpha}^{\alpha}\int h_2(t_1,\tau_2)e^{j\omega\tau_1+j\omega\tau_2}d\tau_1 d\tau_2 \\
&= \frac{A^2}{4}e^{j2\omega t}H_2(\omega,\omega)+\frac{A^2}{4}e^{-j\omega t}H_2(\omega,-\omega)+\frac{A^2}{4}e^{j2\omega t}H_2(-\omega,\omega)+\frac{A^2}{4}e^{-j\omega t}H_2(-\omega,-\omega) \\
&= \frac{A^2}{4}e^{j2\omega t}H_2(\omega,\omega)+\frac{A^2}{4}H_2(\omega,-\omega)+\text{conjugate terms}
\end{aligned}
\tag{2.19}
$$

$$
\begin{aligned}
x_3(t) &= \int_{-\alpha}^{\alpha}\iint h_3(\tau_1,\tau_2,\tau_3)\left[\frac{A}{2}e^{j\omega(t-\tau_1)}+\frac{A}{2}e^{-j\omega(t-\tau_1)}\right]*\left[\frac{A}{2}e^{j\omega(t-\tau_2)}+\frac{A}{2}e^{-j\omega(t-\tau_2)}\right] \\
&*\left[\frac{A}{2}e^{j\omega(t-\tau_3)}+\frac{A}{2}e^{-j\omega(t-\tau_3)}\right]d\tau_1 d\tau_2 d\tau_3 \\
&= \int_{-\alpha}^{\alpha}\iint h_3(\tau_1,\tau_2,\tau_3)[\left[\frac{A^2}{4}e^{j\omega(2t-\tau_1-\tau_2)}\frac{A^2}{4}e^{-j\omega\tau_1+j\omega\tau_2}+\frac{A^2}{4}e^{j\omega\tau_1-j\omega\tau_2}\right. \\
&\left.+\frac{A^2}{4}e^{-2j\omega t+j\omega\tau_1+j\omega\tau_2}\right]*\left[\frac{A}{2}e^{j\omega(t-\tau_3)}+\frac{A}{2}e^{-j\omega(t-\tau_3)}\right]d\tau_1 d\tau_2 d\tau_3 \\
&= \int_{-\alpha}^{\alpha}\iint h_3(\tau_1,\tau_2,\tau_3)[\frac{A^3}{8}e^{j\omega(3t-\tau_1-\tau_2-\tau_3)}+\frac{A^3}{8}e^{j\omega(t-\tau_1-\tau_2+\tau_3)}+\frac{A^3}{8}e^{j\omega(t-\tau_1+\tau_2-\tau_3)} \\
&+\frac{A^3}{8}e^{j\omega(-t-\tau_1+\tau_2+\tau_3)}+\frac{A^3}{8}e^{j\omega(t+\tau_1-\tau_2-\tau_3)}+\frac{A^3}{8}e^{j\omega(-t+\tau_1-\tau_2+\tau_3)} \\
&+\frac{A^3}{8}e^{j\omega(-t+\tau_1+\tau_2-\tau_3)}+\frac{A^3}{8}e^{j\omega(-3t+\tau_1+\tau_2+\tau_3)}]d\tau_1 d\tau_2 d\tau_3 \\
&= \frac{A^3}{8}e^{j3\omega t}H_3(\omega,\omega,\omega)+\frac{3A^3}{8}e^{j\omega t}H_3(\omega,\omega,-\omega) \\
&+\frac{3A^3}{8}e^{-j\omega t}H_3(\omega,-\omega,-\omega)+\frac{A^3}{8}e^{-j3\omega t}H_3(-\omega,-\omega,-\omega) \\
&= \frac{A^3}{8}e^{j3\omega t}H_3(\omega,\omega,\omega)+\frac{3A^3}{8}e^{j\omega t}H_3(\omega,\omega,-\omega)+\text{conjugate terms}
\end{aligned}
\tag{2.20}
$$

In equations (2.18)-(2.20), the term $H_1(\omega_1)$ is the first order Frequency Response Function of the system and can be readily shown to be given by (Schetzen, 1980)

$$H_1(\omega_1) = \frac{1}{\sqrt{(k_1 - m\omega^2)^2 + (c\omega)^2}} \tag{2.21}$$

and the higher order FRFs, $H_2(\omega_1,\omega_2)$ and $H_3(\omega_1,\omega_2,\omega_3)$ can be expressed in terms of the first order FRF $H_1(\omega_1)$ as given below (Chatterjee and Vyas, 1999)

$$H_2(\omega_1,\omega_2) = -k_2 H_1(\omega_1)H_1(\omega_2)H_1(\omega_1+\omega_2)$$

$$H_3(\omega_1,\omega_2,\omega_3) = H_1(\omega_1)H_1(\omega_2)H_1(\omega_3)H_1(\omega_1+\omega_2+\omega_3)* \left[\frac{2k_2^{\,2}}{3}\{H_1(\omega_1+\omega_2)+H_1(\omega_2+\omega_3)+H_1(\omega_3+\omega_1)\}-k_3\right] \tag{2.22}$$

Collecting terms of identical frequency, in x_1, x_2, x_3 from equations (2.18) - (2.20), gives the overall response $x(t)$ in terms of its various frequency components as

$$x(t) = z_0 + |z(\omega_1)|\cos(\omega_1 t + \phi_1) + |z(2\omega_1)|\cos(2\omega_1 t + \phi_2) + |z(3\omega_1)|\cos(3\omega_1 t + \phi_3) + \ldots \tag{2.23}$$

where

$$z(\omega_1) = AH_1(\omega_1) + \frac{3}{4}A^3 H_3(\omega_1,\omega_1,-\omega_1) + \frac{15}{16}A^5 H_5(\omega_1,\omega_1,\omega_1-\omega_1,-\omega_1) + \text{higher order terms}$$

$$z(2\omega_1) = \frac{A^2}{2}H_2(\omega_1,\omega_1) + \frac{A^4}{4}H_4(\omega_1,\omega_1,\omega_1,-\omega_1) + \ldots\ldots \tag{2.24}$$

$$z(3\omega_1) = \frac{A^3}{4}H_3(\omega_1,\omega_1,\omega_1) + \frac{5A^5}{16}H_5(\omega_1,\omega_1,\omega_1,-\omega_1,-\omega_1) + \ldots\ldots$$

$$z_0 = A^2 H_2(\omega_1,-\omega_1) + \frac{3}{4}A^4 H_4(\omega_1,\omega_1,-\omega_1,\omega_1) + \ldots\ldots$$

Restricting, to the first to third FRFs alone (terms $H_1(\omega_1)$ to $H_3(\omega_1,\omega_1,-\omega_1)$, i.e. excluding $H_4(\omega_1,\omega_1,-\omega_1,\omega_1)$, $H_5(\omega_1,\omega_1,\omega_1,-\omega_1,-\omega_1)$ and other higher order FRFs), in equations (2.24), it can be noted, from equations (2.21) and (2.22), that the maximum response at frequencies ω_1, $2\omega_1$, $3\omega_1$ will occur respectively when these frequencies are equal to the linear natural frequency ($\sqrt{k_1/m}$).

2.2.2 Response to Two Tone Excitation

For a two-tone harmonic excitation,

$$f(t) = A\cos w_1(t) + B\cos\omega_2 t \tag{2.25}$$

of the system described by equation (2.10), (with spring force including terms upto cubic only), the various frequency components of the response $x(t)$ can be shown to be

$$z(\omega_1) = AH_1(\omega_1) + \frac{3}{4}A^3H_3(\omega_1,\omega_1,-\omega_1) + \frac{3}{2}AB^2H_3(\omega_1,\omega_2,-\omega_2) + \frac{15}{16}A^5H_5(\omega_1,\omega_1,\omega_1-\omega_1,-\omega_1)$$
$$+\frac{5}{16}AB^4H_5(\omega_1,\omega_2,\omega_2-\omega_2,-\omega_2) + \frac{15}{8}A^3B^2H_5(\omega_1,\omega_1,-\omega,\omega_2,-\omega_2)$$

$$z(\omega_2) = BH_1(\omega_2) + \frac{3}{4}B^3H_3(\omega_2,\omega_2,-\omega_2) + \frac{3}{2}BA^2H_3(\omega_1,\omega_2,-\omega_2) + \frac{15}{16}B^5H_5(\omega_2,\omega_2,\omega_2-\omega_2,-\omega_2)$$
$$+\frac{5}{16}BA^4H_5(\omega_1,\omega_1,-\omega_1-\omega_1,-\omega_2) + \frac{15}{8}B^3A^2H_5(\omega_2,\omega_2,-\omega_2,\omega_1,-\omega_1)$$

$$z(2\omega_1) = \frac{A^2}{2}H_2(\omega_1,\omega_1) + \frac{A^2}{2}H_4(\omega_1,\omega_1,\omega_1,-\omega_1) + \frac{3}{2}A^2B^2H_4(\omega_1,\omega_1,\omega_2,\omega_2) + \ldots$$

$$z(2\omega_2) = \frac{B^2}{2}H_2(\omega_1,\omega_1) + \frac{B^2}{2}H_4(\omega_2,\omega_2,\omega_2,-\omega_2) + \frac{3}{2}A^2B^2H_4(\omega_1,-\omega_1,\omega_2,\omega_2) + \ldots$$

$$z(3\omega_1) = \frac{A^3}{4}H_3(\omega_1,\omega_1,\omega_1) + \frac{5}{16}A^5H_5(\omega_1,\omega_1,\omega_1-\omega_1,-\omega_1) + \frac{5}{4}A^3B^2H_5(\omega_1,\omega_1,\omega_1,\omega_2,-\omega_2) + \ldots$$

$$z(3\omega_2) = \frac{B^3}{4}H_3(\omega_2,\omega_2,\omega_2) + \frac{5}{16}B^5H_5(\omega_2,\omega_2,\omega_2,\omega_2,-\omega_2) + \frac{5}{4}B^3A^2H_5(\omega_2,\omega_2,\omega_2,\omega_1,-\omega_1) + \ldots$$

$$z(\omega_1+\omega_2) = ABH_2(\omega_1,\omega_2) + \frac{3}{2}A^3BH_4(\omega_1,\omega_1,-\omega_1,\omega_2) + \frac{3}{2}AB^3H_4(\omega_1,\omega_2,-\omega_2,-\omega_2) + \ldots$$

$$z(2\omega_1+\omega_2) = \frac{3}{4}A^2BH_3(\omega_1,\omega_1,\omega_2) + \frac{5}{4}A^4BH_5(\omega_1,\omega_1,\omega_1,-\omega_1,\omega_2) + \frac{15}{8}A^2B^3H_5(\omega_1,\omega_1,\omega_2,\omega_2,-\omega_2) + \ldots$$

$$z(2\omega_1-\omega_2) = \frac{3}{4}A^2BH_3(\omega_1,\omega_1,-\omega_2) + \frac{5}{4}A^4BH_5(\omega_1,\omega_1,\omega_1,-\omega_1,-\omega_2) + \frac{15}{8}A^2B^3H_5(\omega_1,\omega_1,\omega_2,-\omega_2,-\omega_2) +$$

$$z(2\omega_2+\omega_1) = \frac{3}{4}B^2AH_3(\omega_1,\omega_1,\omega_2) + \frac{5}{4}AB^4H_5(\omega_1,\omega_2,\omega_2,\omega_2,-\omega_2) + \frac{15}{8}A^3B^2H_5(\omega_1,\omega_1,-\omega_1,\omega_2,\omega_2) + \ldots$$

$$z(2\omega_2-\omega_1) = \frac{3}{4}B^2AH_3(-\omega_1,\omega_2,\omega_2) + \frac{5}{4}B^4AH_5(-\omega_1,\omega_2,\omega_2,\omega_2,-\omega_2) + \frac{15}{8}A^3B^2H_5(\omega_1,-\omega_1,-\omega_1,\omega_2,\omega_2,$$

$$z_0 = A^2H_2(\omega_1,-\omega_1) + B^2H_2(\omega_2,-\omega_2) + \frac{3}{4}A^4H_4(\omega_1,\omega_1,-\omega_1,-\omega_1) \tag{2.26}$$
$$+6A^2B^2H_4(\omega_1,-\omega_1,\omega_2,-\omega_2) + \frac{3}{4}B^4H_4(\omega_2,\omega_2,-\omega_2,-\omega_2) + \ldots$$

2.2.3 Response to Three Tone Excitation

Similarly, for a three-tone harmonic excitation,

$$f(t) = A\cos\omega_1(t) + B\cos\omega_2 t + C\cos\omega_3 t \tag{2.27}$$

the frequency components of the response can be worked out to be

$$\begin{aligned}
z(\omega_1) &= AH_1(\omega_1) + \frac{3}{4}A^3H_3(\omega_1,\omega_1,-\omega_1) + \frac{3}{2}AB^2H_3(\omega_1,\omega_2,-\omega_2) + \frac{3}{2}AC^2H_3(\omega_1,\omega_2,-\omega_3) \\
&+ \frac{15}{16}A^5H_5(\omega_1,\omega_1,\omega_1-\omega_1,-\omega_1) + \frac{5}{16}AB^4H_5(\omega_1,\omega_2,\omega_2-\omega_2,-\omega_2) \\
&+ \frac{5}{16}AC^4H_5(\omega_1,\omega_3,\omega_3-\omega_3,-\omega_3) + \frac{15}{8}A^3B^2H_5(\omega_1,\omega_1,-\omega_1,\omega_2,-\omega_2) \\
&+ \frac{15}{8}A^3C^2H_5(\omega_1,\omega_1,-\omega_1,\omega_3,-\omega_3) + \frac{15}{4}AB^2C^2H_5(\omega_1,\omega_2,-\omega_2,\omega_3,-\omega_3) + \ldots \\
z(\omega_2) &= BH_1(\omega_2) + \frac{3}{4}B^3H_3(\omega_2,\omega_2,-\omega_2) + \frac{3}{2}BA^2H_3(\omega_1,-\omega_1,-\omega_2) + \frac{3}{2}BC^2H_3(\omega_2,\omega_3,-\omega_3) \\
&+ \frac{15}{16}B^5H_5(\omega_2,\omega_2,\omega_2-\omega_2,-\omega_2) + \frac{5}{16}BA^4H_5(\omega_1,\omega_1,-\omega_1-\omega_1,\omega_2) \\
&+ \frac{5}{16}BC^4H_5(\omega_2,\omega_3,\omega_3-\omega_3,-\omega_3) + \frac{15}{8}B^3A^2H_5(\omega_2,\omega_2,-\omega_2,\omega_1,-\omega_1) \\
&+ \frac{15}{8}B^3C^2(\omega_2,\omega_2,-\omega_2,\omega_3,-\omega_3) + \frac{15}{4}A^2BC^2H_5(\omega_1,-\omega_1,\omega_2,\omega_3,-\omega_3) + \ldots\ldots \\
z(\omega_3) &= CH_1(\omega_3) + \frac{3}{4}C^3H_3(\omega_3,\omega_3,-\omega_3) + \frac{3}{2}CA^2H_3(\omega_1,-\omega_1,-\omega_3) \\
&+ \frac{3}{2}CB^2H_3(\omega_2,-\omega_2,\omega_3) + \ldots \\
z(2\omega_1) &= \frac{A^2}{2}H_2(\omega_1,\omega_1) + \frac{A^2}{2}H_4(\omega_1,\omega_1,\omega_1,-\omega_1) + \frac{3}{2}A^2B^2H_4(\omega_1,\omega_1,\omega_2,-\omega_2) \\
&+ \frac{3}{2}A^2C^2H_4(\omega_1,\omega_1,\omega_3,-\omega_3) + \ldots \\
z(2\omega_2) &= \frac{B^2}{2}H_2(\omega_2,\omega_2) + \frac{B^4}{2}H_4(\omega_2,\omega_2,\omega_2,-\omega_2) + \frac{3}{2}A^2B^2H_4(\omega_1,-\omega_1,\omega_2,\omega_2) \\
&+ \frac{3}{2}B^2C^2H_4(\omega_2,\omega_2,\omega_3,-\omega_3) + \ldots \\
z(2\omega_3) &= \frac{C^2}{2}H_2(\omega_3,\omega_3) + \frac{C^4}{2}H_4(\omega_3,\omega_3,\omega_3,-\omega_3) + \frac{3}{2}A^2C^2H_4(\omega_1,-\omega_1,\omega_3,\omega_3) \\
&+ \frac{3}{2}B^2C^2H_4(\omega_2,-\omega_2,\omega_3,\omega_3) + \ldots
\end{aligned} \tag{2.28}$$

$$z(3\omega_1)=\frac{A^3}{4}H_3(\omega_1,\omega_1,\omega_1)+\frac{5}{16}A^5H_5(\omega_1,\omega_1,\omega_1,-\omega_1,-\omega_1)$$
$$+\frac{5}{4}A^3B^2H_5(\omega_1,\omega_1,\omega_1,\omega_2,-\omega_2)+\frac{5}{4}A^3C^2H_5(\omega_1,\omega_1,\omega_1,\omega_3,-\omega_3)+\ldots$$

$$z(3\omega_2)=\frac{B^3}{4}H_3(\omega_2,\omega_2,\omega_2)+\frac{5}{16}B^5H_5(\omega_2,\omega_2,\omega_2,\omega_2,-\omega_2)$$
$$+\frac{5}{4}B^3A^2H_5(\omega_2,\omega_2,\omega_2,\omega_1,-\omega_1)+\ldots$$

$$z(3\omega_3)=\frac{C^3}{4}H_3(\omega_3,\omega_3,\omega_3)+\frac{5}{16}C^5H_5(\omega_3,\omega_3,\omega_3,\omega_3,-\omega_3)$$
$$+\frac{5}{4}C^3A^2H_5(\omega_3,\omega_3,\omega_3,\omega_1,-\omega_1)+\frac{5}{4}C^3B^2H_5(\omega_3,\omega_3,\omega_3,\omega_2,-\omega_2)+\ldots$$

$$z(\omega_1+\omega_2)=ABH_2(\omega_1,\omega_2)+\frac{3}{2}A^3BH_4(\omega_1,\omega_1,-\omega_1,\omega_2)+\frac{3}{2}AB^3H_4(\omega_1,\omega_2,-\omega_2,-\omega_2)$$
$$+ABC^2H_4(\omega_1,\omega_2,\omega_3,-\omega_3)+\ldots$$

$$z(\omega_2+\omega_3)=BCH_2(\omega_2,\omega_3)+\frac{3}{2}B^3CH_4(\omega_2,\omega_2,-\omega_2,\omega_3)+\frac{3}{2}AB^3H_4(\omega_1,\omega_2,\omega_2,-\omega_2)$$
$$+3A^2BCH_4(\omega_1,-\omega_1,\omega_2,\omega_3)+\ldots$$

$$z(\omega_1+\omega_3)=ACH_2(\omega_1,\omega_3)+\frac{3}{2}A^3CH_4(\omega_1,\omega_1,-\omega_1,\omega_3)+\frac{3}{2}AC^3H_4(\omega_1,\omega_3,\omega_3,-\omega_3)$$
$$+3AB^2CH_4(\omega_1,\omega_3,\omega_2,-\omega_2)+\ldots$$

$$z(\omega_1-\omega_2)=ABH_2(\omega_1,-\omega_2)+\frac{3}{2}A^3BH_4(\omega_1,\omega_1,-\omega_1,-\omega_2)+\frac{3}{2}AB^3H_4(\omega_1,\omega_2,-\omega_2,-\omega_2)$$
$$+3ABC^2H_4(\omega_1,-\omega_2,\omega_3,-\omega_3)+\ldots$$

$$z(\omega_1+\omega_2+\omega_3)=\frac{3}{2}ABCH_3(\omega_1,\omega_2,\omega_3)+\frac{15}{4}A^3BCH_5(\omega_1,\omega_1,-\omega_1,\omega_2,\omega_3)$$
$$+\frac{15}{4}AB^3CH_5(\omega_1,\omega_2,\omega_2,-\omega_2,\omega_3)+\frac{15}{4}ABC^3H_5(\omega_1,\omega_2,\omega_3,\omega_3,-\omega_3)$$
$$+\text{higher order terms}$$

$$z(2\omega_1+\omega_2)=\frac{3}{4}A^2BH_3(\omega_1,\omega_1,\omega_2)+\frac{5}{4}A^4BH_5(\omega_1,\omega_1,\omega_1,-\omega_1,\omega_2)$$
$$+\frac{15}{8}A^2B^3H_5(\omega_1,\omega_1,\omega_2,\omega_2,-\omega_2)+\ldots$$

$$z(2\omega_1-\omega_2)=\frac{3}{4}A^2BH_3(\omega_1,\omega_1,-\omega_2)+\frac{5}{4}AB^4H_5(\omega_1,\omega_2,\omega_2,-\omega_1,-\omega_2)$$
$$+\frac{15}{8}A^2B^3H_5(\omega_1,\omega_1,\omega_2,-\omega_2,-\omega_2)+\frac{15}{8}A^2BC^2H_5(\omega_1,\omega_1,\omega_2,\omega_3,-\omega_3)+\ldots$$

$$z(2\omega_2+\omega_1)=\frac{3}{4}B^2AH_3(\omega_1,\omega_2,\omega_2)+\frac{5}{4}AB^4H_5(\omega_1,\omega_2,\omega_2,\omega_2,-\omega_2)$$
$$+\frac{15}{8}A^3B^2H_5(\omega_1,\omega_1,-\omega_1,\omega_2,\omega_2)+\frac{15}{8}AB^2C^2H_5(\omega_1,\omega_2,\omega_2,\omega_3,-\omega_3)+\ldots$$

$$z(2\omega_2-\omega_1)=\frac{3}{4}B^2AH_3(-\omega_1,\omega_2,\omega_2)+\frac{5}{4}B^4AH_5(-\omega_1,\omega_2,\omega_2,\omega_2,-\omega_2)$$
$$+\frac{15}{8}A^3B^2H_5(\omega_1,-\omega_1,-\omega_1,\omega_2,\omega_2)+\frac{15}{8}AB^2C^2H_5(-\omega_1,\omega_2,\omega_2,\omega_3,-\omega_2)+\ldots$$

$$z(2\omega_2+\omega_3)=\frac{3}{4}A^2CH_3(\omega_1,\omega_2,\omega_3)+\frac{5}{4}A^4CH_5(\omega_1,\omega_1,\omega_1,\omega_1,-\omega_3)$$
$$+\frac{5}{4}A^2B^2CH_5(\omega_1,\omega_1,\omega_2,-\omega_2,\omega_3)+\frac{5}{4}A^2C^3H_5(\omega_1,\omega_1,\omega_3,\omega_3,-\omega_3)+\ldots.$$

$$z(2\omega_1-\omega_3)=\frac{3}{4}A^2CH_3(\omega_1,\omega_1,-\omega_3)+\frac{5}{4}A^4CH_5(\omega_1,\omega_1,\omega_1,-\omega_1,-\omega_3)$$
$$+\frac{5}{4}A^2B^2CH_5(\omega_1,\omega_1,\omega_2,-\omega_2,-\omega_3)+\frac{5}{4}A^2C^3H_5(\omega_1,\omega_1,\omega_3,\omega_3,-\omega_3)+\ldots.$$

$$z_0=A^2H_2(\omega_1,-\omega_1)+B^2H_2(\omega_2,-\omega_2)+C^2H_2(\omega_3,-\omega_3)$$
$$+\frac{3}{4}A^4H_4(\omega_1,\omega_1,-\omega_1,-\omega_1)+6A^2C^2H_4(\omega_1,-\omega_1,\omega_3,-\omega_3)+\frac{3}{4}B^4H_4(\omega_2,\omega_2,-\omega_2,-\omega_2)$$
$$+6B^2C^2H_4(\omega_2,-\omega_{22},\omega_3,-\omega_3)+\frac{3}{4}C^4H_4(\omega_3,\omega_3,-\omega_3,-\omega_3)+\ldots$$

It can be seen, from equations (2.24), (2.26), (2.28), that for a system with polynomial type of nonlinearity (equation 2.10), excited by harmonic forces, the response comprises of components at frequencies, which are multiples and various linear combinations of the excitation frequencies. It is to be noted that, if the system is linear, the response would contain frequency components at the excitation frequencies ω_1, ω_2, ω_3 only. This fact is employed in the proposed crack detection procedure, which is discussed in the next chapter.

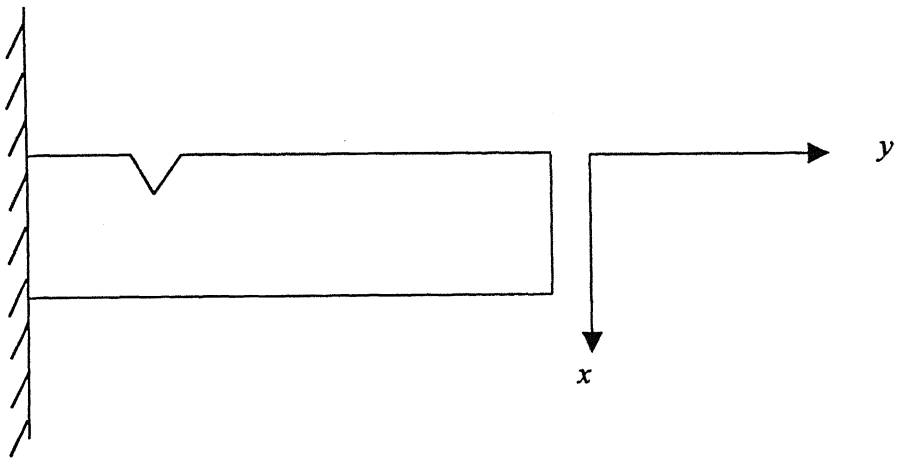

Fig. 2.1 Beam with a breathing crack

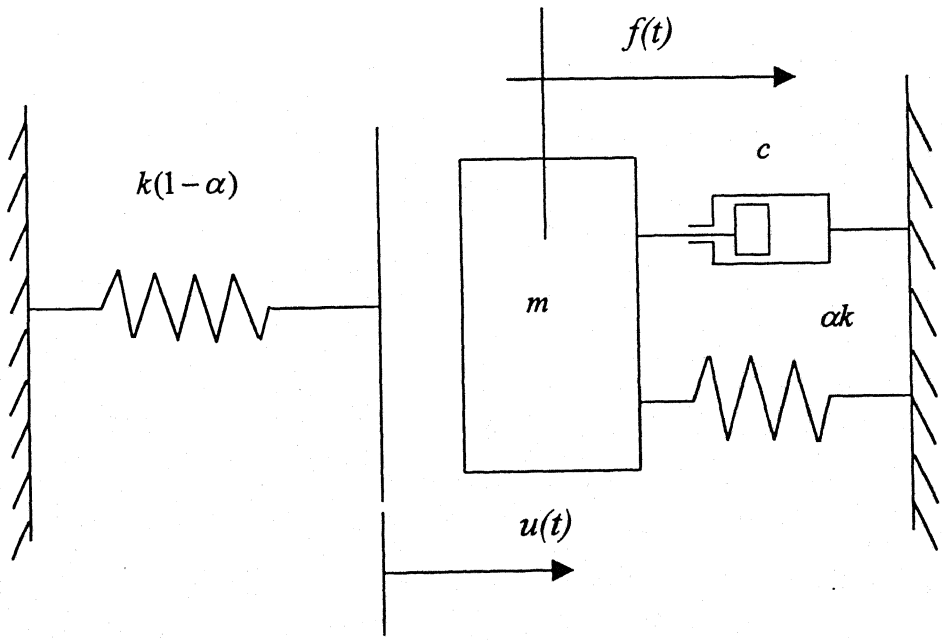

Fig. 2.2 The bilinear model

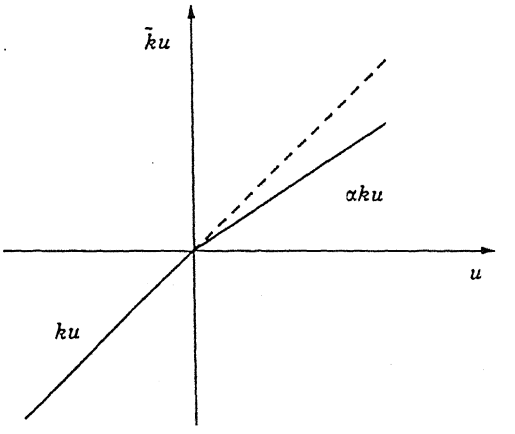

Fig. 2.3 Piecewise restoring force

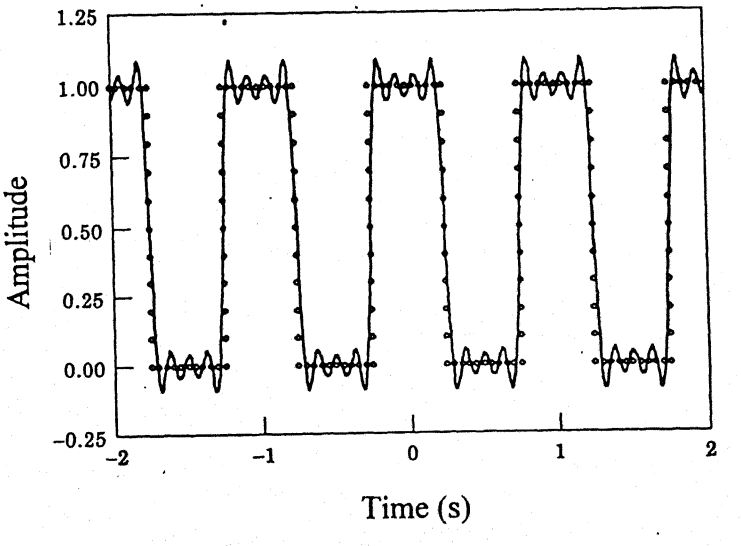

Fig. 2.4 Square-wave approximation of restoring force

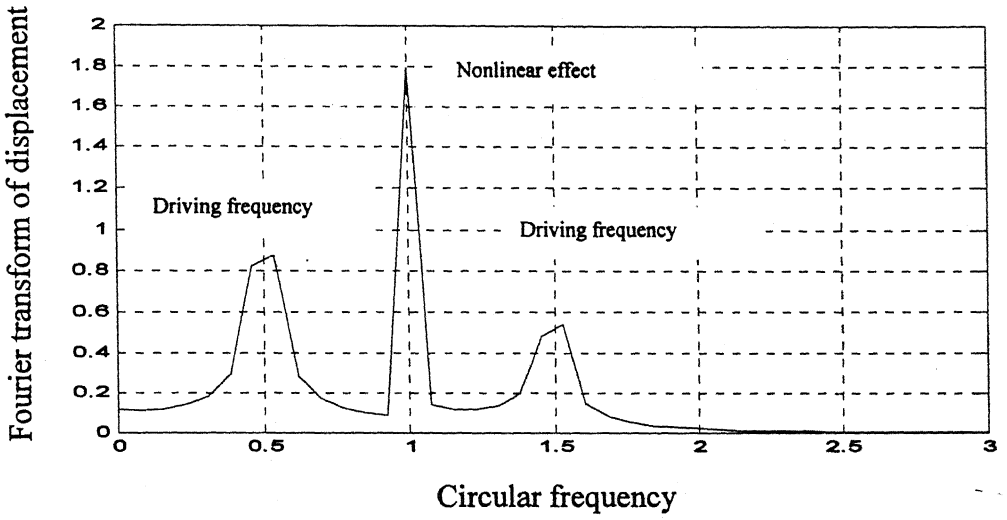

Fig 2.5 The Fourier transform of the steady state time history (Ref: Sundermeyer and Weaver, 1995)

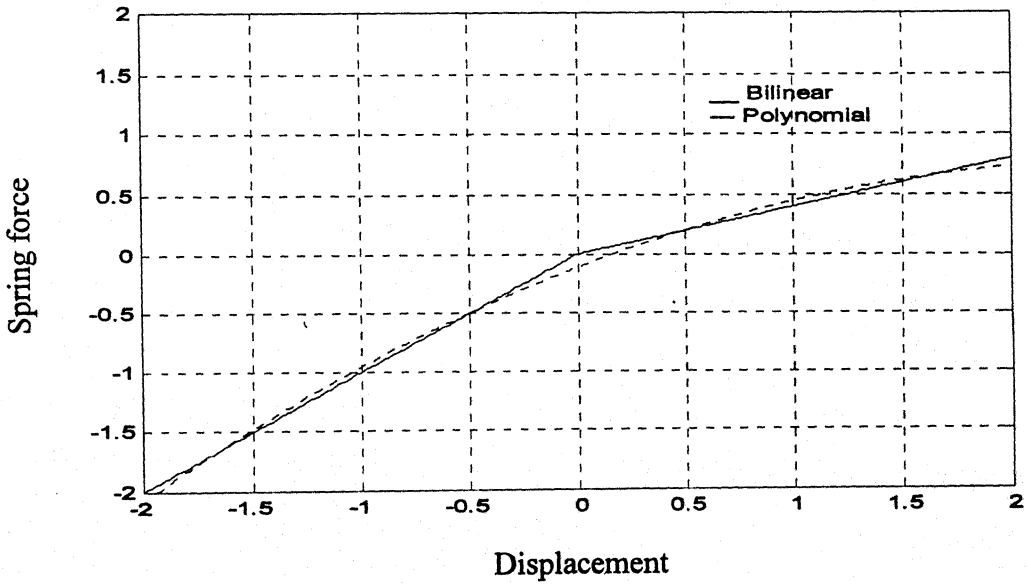

Fig. 2.6 Spring forces of bilinear and polynomial models

CHAPTER 3

CRACK DETECTION PROCEDURE AND NUMERICAL SIMULATION

The difference between the response of a linear system and that of a nonlinear system, to single and multi-tone harmonic excitation is the basis for the proposed crack detection procedure. Inherent assumption is that a beam without crack would behave as a linear single-degree-of-freedom system, in its fundamental mode, while the presence of a crack would make its stiffness bilinear. Further, this bilinear stiffness, approximated through a polynomial, would render the system nonlinear. The harmonic components present in the response of a beam, can therefore be taken as an indicator of the presence of a crack in the beam. Numerical simulation of such systems carried out through MATLAB Simulink models have been discussed in this chapter.

3.1 Numerical Simulation of the Bilinear Model

Numerical simulation has been carried to obtain the response of a system governed by the following equation.

$$m\ddot{x} + c\dot{x} + (k - k_\varepsilon)x = F_0 \sin \omega t \qquad k_\varepsilon \neq 0 \quad for\ x > 0; \qquad k_\varepsilon = 0 \quad for\ x \leq 0 \qquad (3.1)$$

In the above, m, c, k are the mass, damping constant and stiffness of the system, $f(t)$ is the excitation force and k_ε is a stiffness reduction factor introduced to accommodate the crack breathing phenomenon. With reference to Fig.2.1, where the crack is on the upper side of the beam and the displacement axis, x, is positive downwards, the crack opens for $x > 0$ and as a result there is a reduction in stiffness, denoted by $k_\varepsilon \neq 0$. For the remaining half-cycle, when $x \leq 0$, the crack can be treated as closed and therefore causing no reduction in stiffness ($k_\varepsilon = 0$).

Equation (3.1) can be written in nondimensional form as

$$\eta'' + 2\xi\eta' + (1 - \varepsilon)\eta = \sin r\tau \qquad (3.2)$$

where the following parameters are employed

natural frequency, $p = \sqrt{k/m}$; nondimensional time, $\tau = pt$;

nondimensional displacement, $\eta = x/X_{st}$; damping ratio, $\xi = c/2mp$ (3.3)

crack severity ratio, $\varepsilon = k_\varepsilon / mp^2$ frequency ratio $r = \omega / p$

($'$) denotes differentiation with respect to τ.

The MATLAB model, employing fourth order Runge-Kutta algorithm, for response simulation of equation (3.2) is given in Appendix A. Simulation was initially done for a beam without crack, i.e., with $\varepsilon = 0$, in equation (3.2) for all η. Three sets of excitation

(i) single tone $\sin r_1\tau$

(ii) two tone $\sin r_1\tau + \sin r_2\tau$

(iii) three tone $\sin r_1\tau + \sin r_2\tau + \sin r_3\tau$

are given to the system. The time and frequency domain plots of these forces are given in Figs.3.1 (a)-(c). The response in the three cases is given in Figs. 3.2 (a)-(c). As expected for a linear system, the response can be seen to comprise of frequency components at the corresponding excitation frequencies, r_1, r_2, r_3, alone.

The response for a bilinear system, with crack severity ratio $\varepsilon = 0.01$, for the three different sets of excitation of Figs 3.1 (a)-(c), is shown in Figs. 3.3 (a)-(c). In addition to the frequency components at the excitation frequencies, r_1, r_2, r_3, the response also shows response harmonics at combination frequencies, $2r_1, (r_2 - r_1), (r_3 - 2r_1), (2r_2 - r_3)$ and $(r_1 - r_2 + r_3)$.

This response pattern is similar to that described in equations (2.24), (2.26) and (2.28), in the previous chapter, for a system with polynomial type of stiffness nonlinearity. For, a polynomial system, these harmonics are expected to achieve maximum value when the corresponding combinational frequency equals the linear natural frequency, *p*, and since the bilinear system exhibits similar response pattern, in Figs. 3.3 (a)-(c), this fact has been employed in the present study to explore crack detection.

The proposed procedure can be outlined as -

Step 1: Identification of the fundamental frequency, p, through a frequency sweep test.

Step 2: Application of single-tone-excitation, to the system at half of the identified natural frequency, i.e. $r_1 = 0.5$. If the system has developed a crack, the response should indicate the presence of frequency component $2r_1$. The excitation frequency, is kept half the natural frequency, so as to get, $2r_1 = 1$, to get the maximum possible magnification for this frequency component. This should enable detection of small amounts of nonlinearity, which may have developed in the originally linear system.

Step 3: The presence of nonlinearity can be further confirmed (and eliminating the possibility of taking noise as the $2r_1$ frequency component), by providing a second excitation tone at $r_2 = 1.5$ (while keeping r_1 fixed at 0.5), so as to make $(r_2 - r_1) = 1$. This will add a magnified $(r_2 - r_1)$ component to the already existing $2r_1$ component at the natural frequency in the frequency response plot.

Step 4: Further, enhancement of the nonlinear effect can be achieved through addition of a third tone of excitation at frequency $r_3 = 2.0$. This would add $(r_3 - 2r_1), (2r_2 - r_3)$ and $(r_1 - r_2 + r_3)$ components to the already existing $2r_1$ and $(r_2 - r_1)$ components at the natural frequency of the system.

The numerical simulation based on the above scheme was carried out with the expectation that detection of fairly small changes in the system stiffness, consequent to crack development, should be possible. The response simulated for four different values of crack severity factors ε = 0.002, 0.004, 0.006, and 0.008, is shown in Figs. 3.4 – 3.7. The nondimensional excitation forces are similar to those described in Fig. 3.1, with frequencies $r_1 = 0.5$; $r_2 = 1.5$; $r_3 = 2.0$. The damping ratio ξ is kept constant at 0.001, in all these cases. For each case FFT plots for single tone, two tone and three tone excitation have been given. In all cases the presence of a peak at

natural frequency ($r = 1$), with single-tone excitation, indicates the presence of a crack. This peak is enhanced for two tone excitation. The enhancement with addition of the third harmonic tone to excitation causes only a marginal difference in the peak amplitude at the natural frequency. This is explained by the fact that the contribution due to the second and third tone excitation depends on the magnitude of the second and third order coefficients, k_2 and k_3, in the equivalent polynomial stiffness representation $g(x) = k_1 x + k_2 x^2 + k_3 x^3$. It turns out, that for a bilinear system, k_3 is a small quantity in comparison to k_2, resulting in small contributions from the third excitation tone (ref. Eqns. 2.22 and 2.28). This is discussed in more detail in the next section. It can be readily noted from Figs.3.4-3.7, that as the crack severity ratio ε increases, crack identification becomes easier due to the presence of larger peaks at the natural frequency. The influence of damping ratio on the crack detection process is shown in Figs. 3.8-3.10 and as expected for smaller values of damping the response harmonics are magnified making the identification process easier.

3.2 Numerical Simulation of the Equivalent Polynomial Model

The equivalent polynomial model has been obtained by least square curve fitting of the displacement versus spring force plot of the bilinear model. The coefficients k_1, k_2, k_3 of the equivalent polynomial, resulting from this exercise are employed in the equations (2.24), (2.26) and (2.28) to get the response harmonics for single tone, two tone and three tone excitations respectively. The expressions obtained from these equations, for the response at natural frequency ($r = 1$), for the three sets of excitation are produced below.

Single tone ($r_1 = 0.5$):

$$Z(r=1) = \frac{1}{2} H_2(r_1, r_1) + \text{higher order terms}$$

$$\approx -\frac{1}{2} k_2 H_1{}^2(r_1) H_1(2r_1)$$

Two tone ($r_1 = 0.5; r_2 = 1.5$):

$$Z(r=1) = \frac{1}{2} H_2(r_1, r_1) + H_2(-r_1, r_2) + \text{higher order terms}$$

$$\approx -k_2 H_1(2r_1)[\frac{1}{2} H_1{}^2(r_1) + H_1(r_2) H_1(-r_1)]$$

Three tone ($r_1 = 0.5; r_2 = 1.5; r_3 = 2.0$):

$$
\begin{aligned}
Z(r=1) &= \frac{1}{2}H_2(r_1,r_1) + H_2(-r_1,r_2) + \frac{3}{4}H_3(-r_1,-r_1,r_3) \\
&+ \frac{3}{4}H_3(r_2,r_2,-r_3) + \frac{3}{2}H_3(r_1,-r_2,r_3) + \text{higher order terms} \\
&\approx -k_2 H_1(2r_1)[\frac{1}{2}H_1{}^2(r_1) + H_1(r_2)H_1(-r_1)] \\
&+ \frac{3}{4}H_1(-r_1)H_1(-r_1)H_1(r_3)H_1(-2r_1+r_3)[\frac{2k_2{}^2}{3}\{H_1(-2r_1) + 2H_1(-r_1+r_3)\} - k_3] \\
&+ \frac{3}{4}H_1(r_2)H_1(r_2)H_1(r_3)H_1(2r_2-r_3)[\frac{2k_2{}^2}{3}\{H_1(2r_2) + 2H_1(2r_2-r_3)\} - k_3] \\
&+ \frac{3}{2}H_1(r_1)H_1(-r_2)H_1(r_3)H_1(r_1-r_2+r_3) \\
&*[\frac{2k_2{}^2}{3}\{H_1(r_1-r_2) + H_1(-r_2+r_3) + H_1(r_1+r_3)\} - k_3]
\end{aligned}
\qquad (4.6)
$$

These response harmonics can also be obtained through Runge-Kutta simulation of the equivalent polynomial system. The MATLAB model for this purpose is given in Appendix 2.

It is to be noted that the values of the equivalent coefficients k_1, k_2, k_3 are dependent on the range of displacement x, in the bilinear model. In the present study, a set of eqivalent polynomial coefficients k_1, k_2, k_3 are obtained for the entire range of displacement x, which are taken to remain constant over an entire cycle oscillation. It is possible to divide the displacement range, x of the bilinear model, into smaller intervals and do curve fitting for individual intervals, to obtain equivalent polynomial coefficients for each displacement interval. This would have increased the computational effort significantly.

The equivalent polynomial model has been created for three crack severity ratios ($\varepsilon = 0.002, 0.004, 0.006$). The coefficients k_1, k_2, k_3 obtained for each case under single tone excitation are

for $\varepsilon = 0.002$ $\quad k_1 = 0.99895081,\ k_2 = 0.00118455,\ k_3 = 0.00014910$

for $\varepsilon = 0.004$ $\quad k_1 = 0.99783879,\ k_2 = 0.00256860,\ k_3 = 0.00053821$

for $\varepsilon = 0.006$ $\quad k_1 = 0.99676018,\ k_2 = 0.00390345,\ k_3 = 0.00082413.$

Here, damping ratio ζ was taken as 0.001 in all three cases.

A comparison of the spring forces of the bilinear and equivalent polynomial models is given in Figs.3.11 (a)-(c), for the three cases.

The response of the equivalent polynomial models, for single, two and three tone excitations, for the chosen crack severity ratios is given in Figs.3.12-3.14. Comparison of these figures with the corresponding ones for the bilinear model (Figs. 3.4, 3.5, 3.6) reveals that for lower values of ε the polynomial model closely represents the response of the bilinear model. For, higher values of ε, the difference between the two increases. It should be possible to improve upon the agreement between the two, through piecewise polynomial approximation, mentioned earlier. The present approximation assumes constant polynomial coefficients, through the entire displacement range. However, it seems sufficient for a qualitative understanding of the response pattern of the bilinear system.

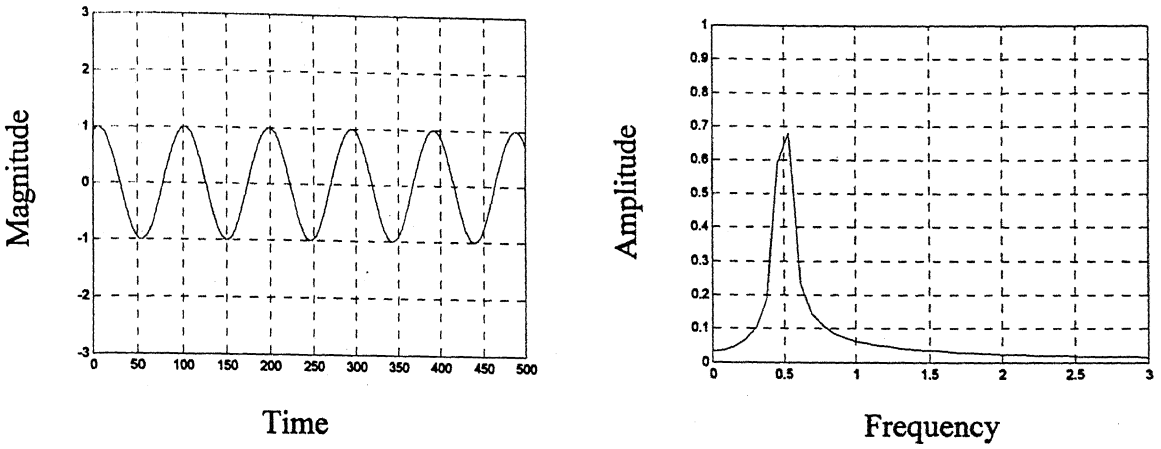

(a) single tone excitation

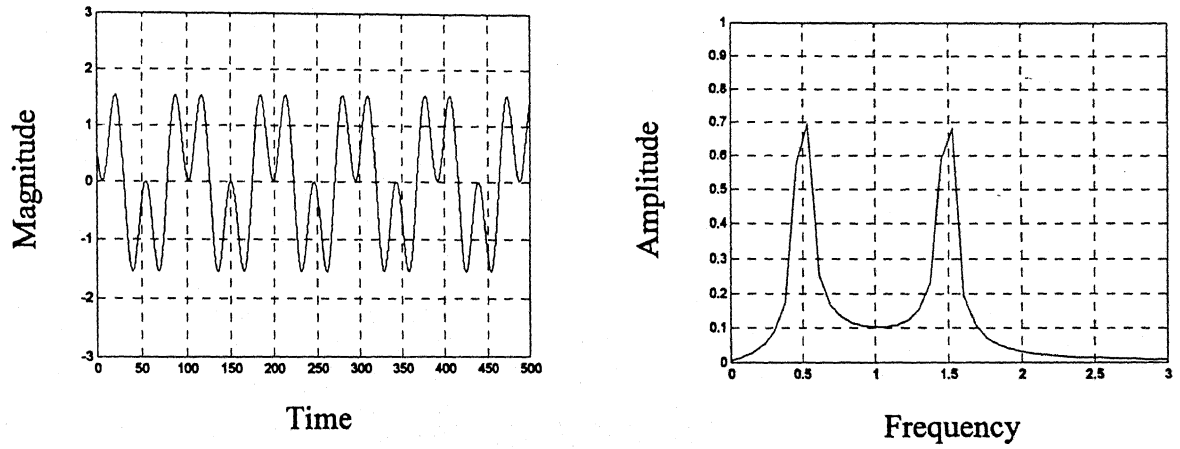

(b) Two tone excitation

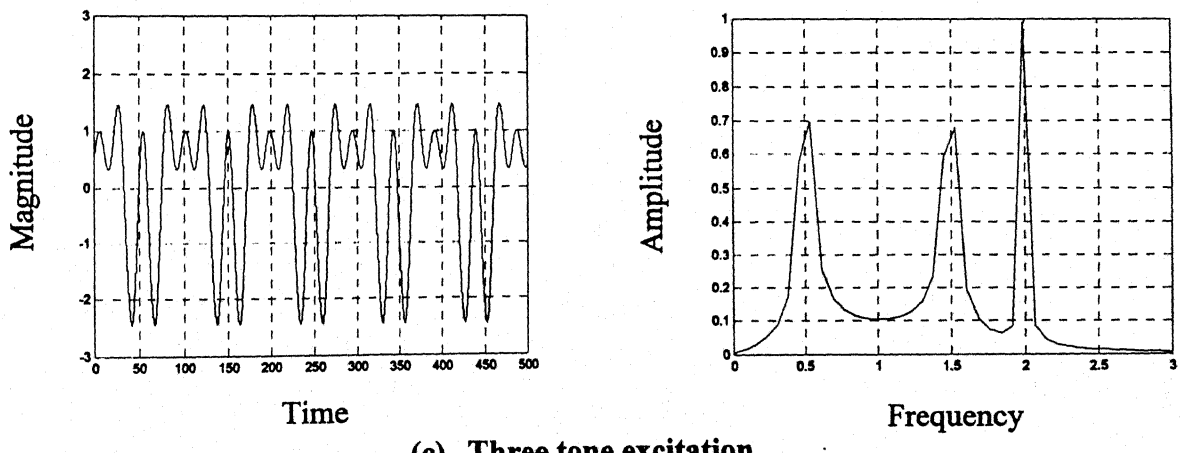

(c) Three tone excitation

Fig. 3.1 Time and frequency domain plots of excitation forces

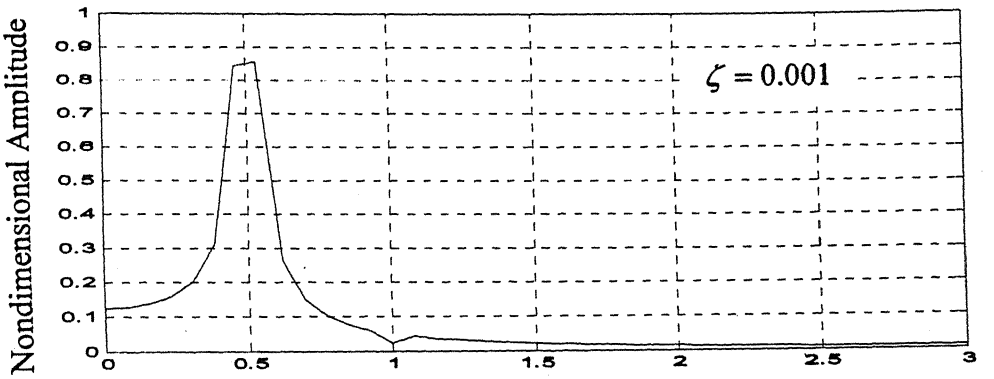

(a) Single tone excitation ($r_1 = 0.5$)

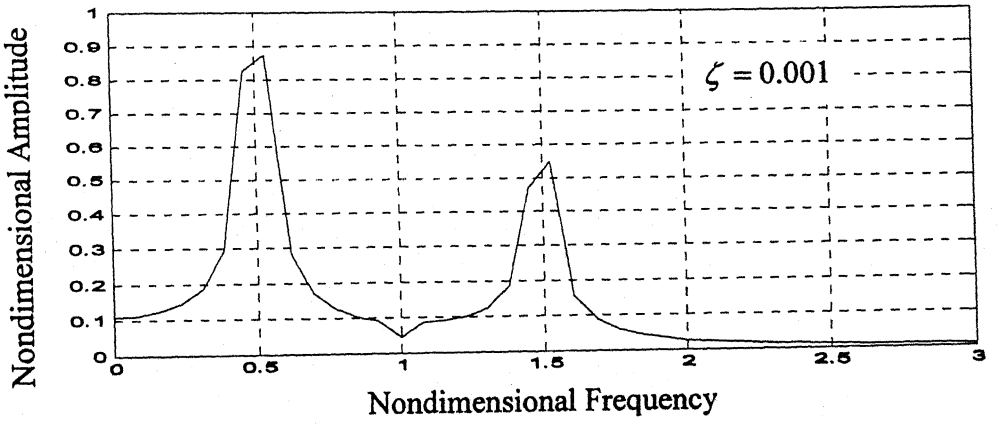

(b) Two tone excitation ($r_1 = 0.5, r_2 = 1.5$)

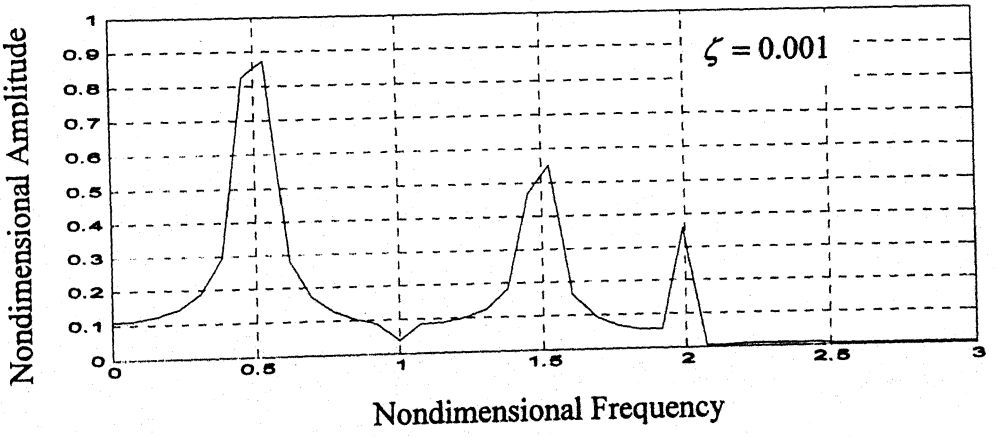

(c) Three tone excitation ($r_1 = 0.5, r_2 = 1.5, r_3 = 2.0$)

Fig. 3.2 Response of beam without crack

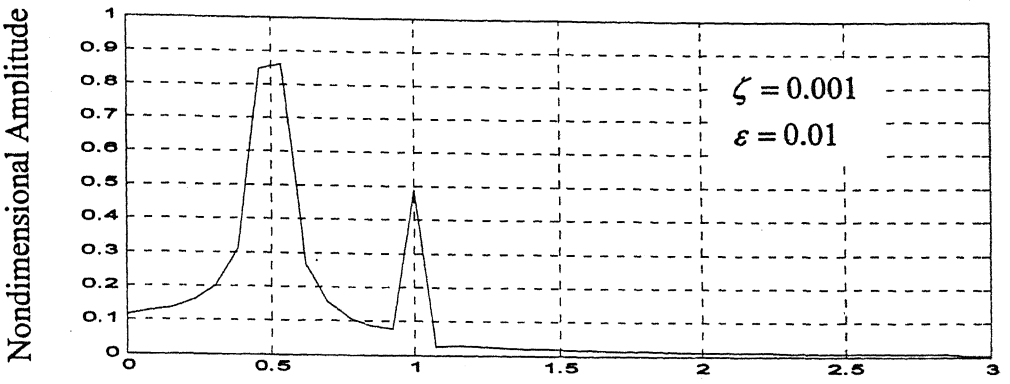

(a) Single tone excitation ($r_1 = 0.5$)

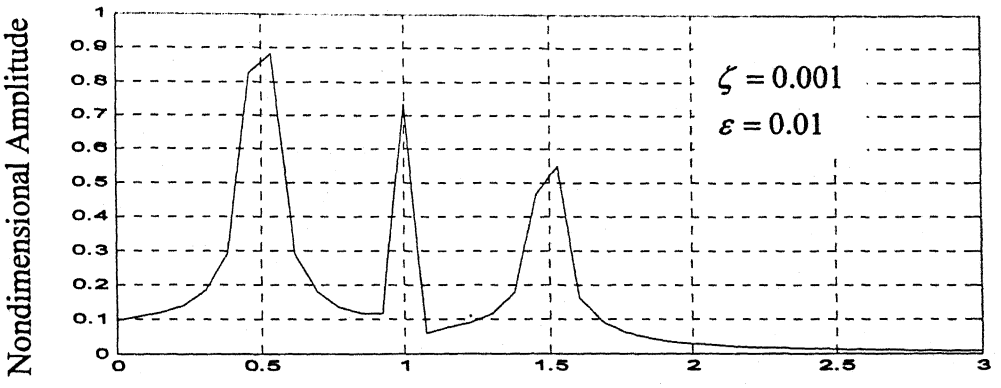

(b) Two tone excitation ($r_1 = 0.5, r_2 = 1.5$)

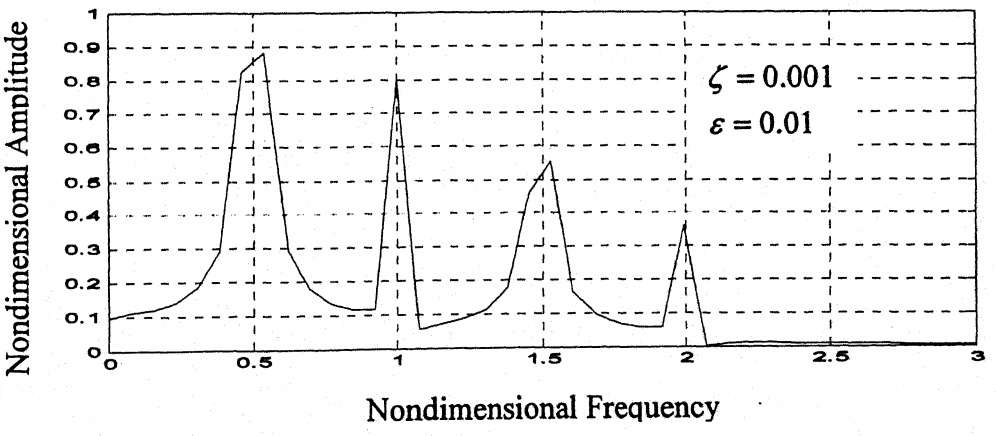

(c) Three tone excitation ($r_1 = 0.5, r_2 = 1.5, r_3 = 2.0$)

Fig. 3.3 Response of a beam with crack
(Crack severity ratio $\varepsilon = 0.01$)

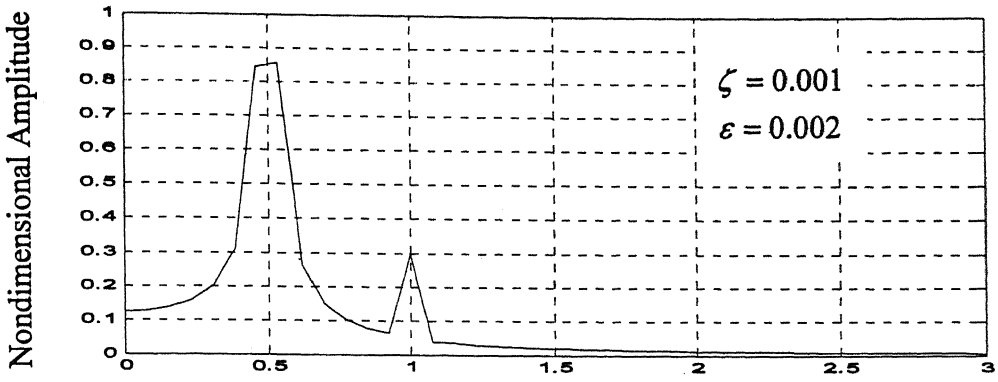

(a) Single tone excitation ($r_1 = 0.5$)

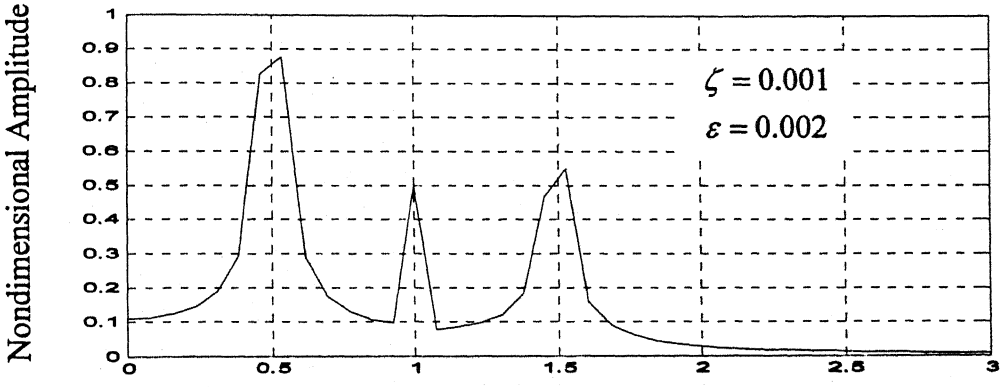

(b) Two tone excitation ($r_1 = 0.5, r_2 = 1.5$)

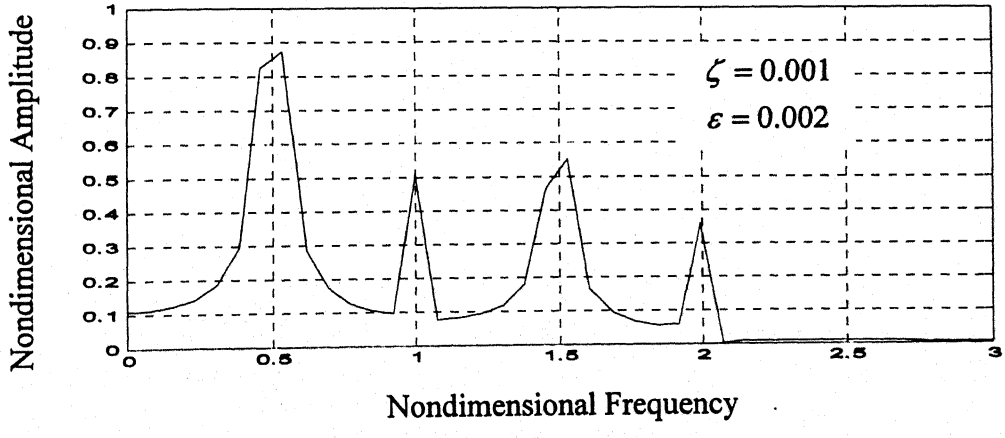

(c) Three tone excitation ($r_1 = 0.5, r_2 = 1.5, r_3 = 2.0$)

Fig. 3.4 Response of a beam with crack
(Crack severity ratio $\varepsilon = 0.002$)

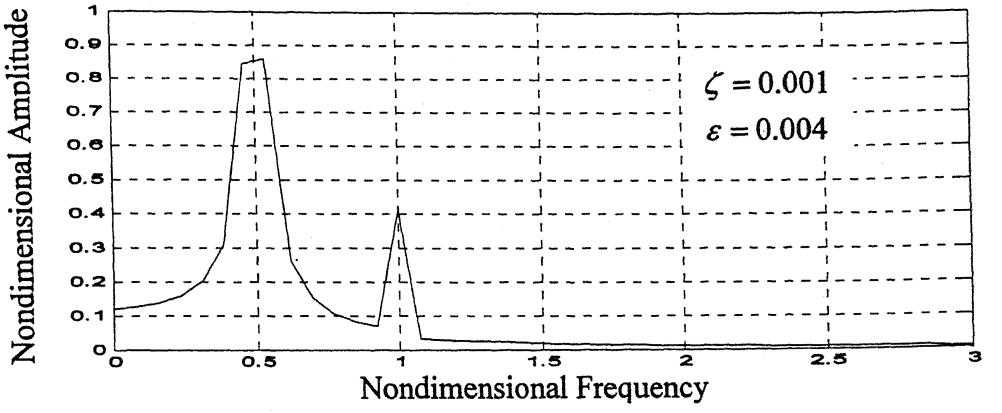

(a) Single tone excitation ($r_1 = 0.5$)

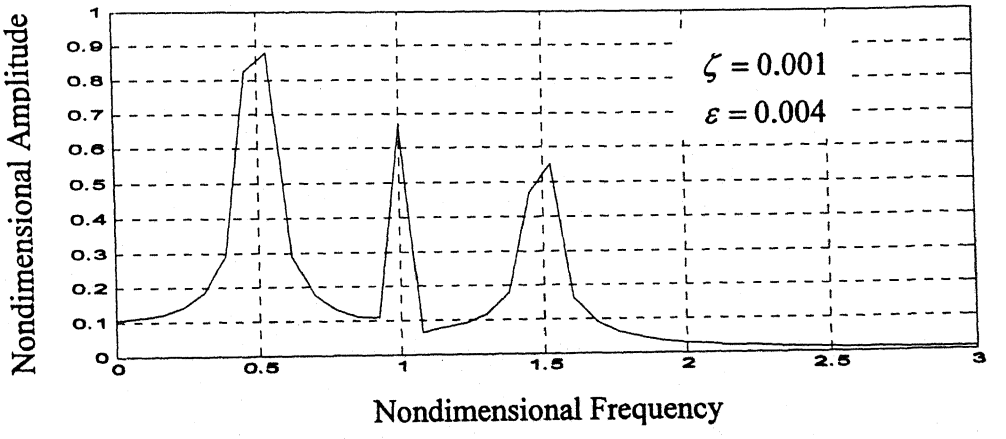

(b) Two tone excitation ($r_1 = 0.5, r_2 = 1.5$)

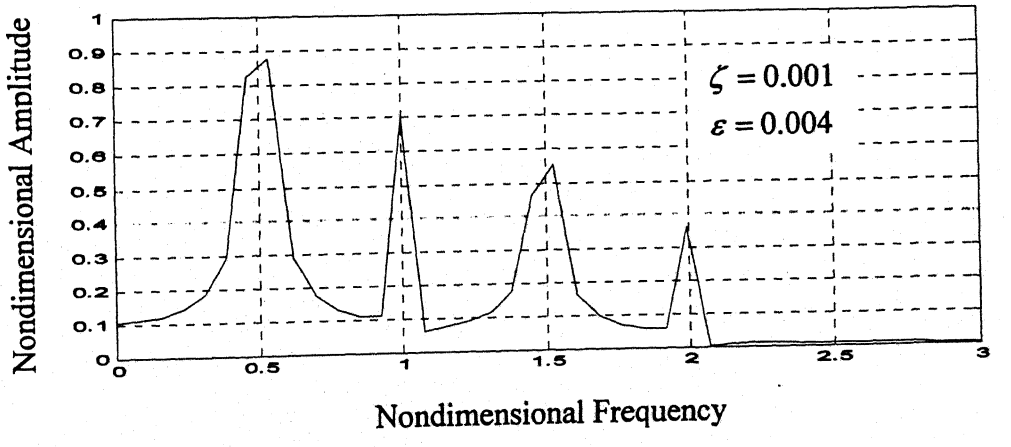

(c) Three tone excitation ($r_1 = 0.5, r_2 = 1.5, r_3 = 2.0$)

Fig. 3.5 Response of a beam with crack
(Crack severity ratio $\varepsilon = 0.004$)

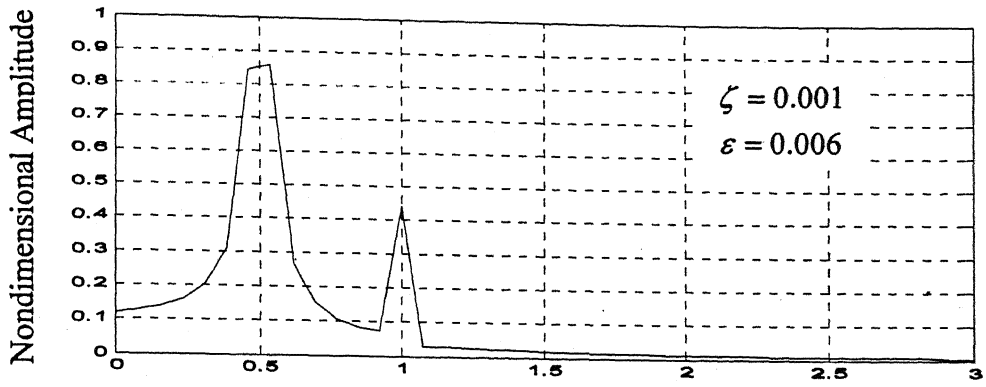

(a) Single tone excitation ($r_1 = 0.5$)

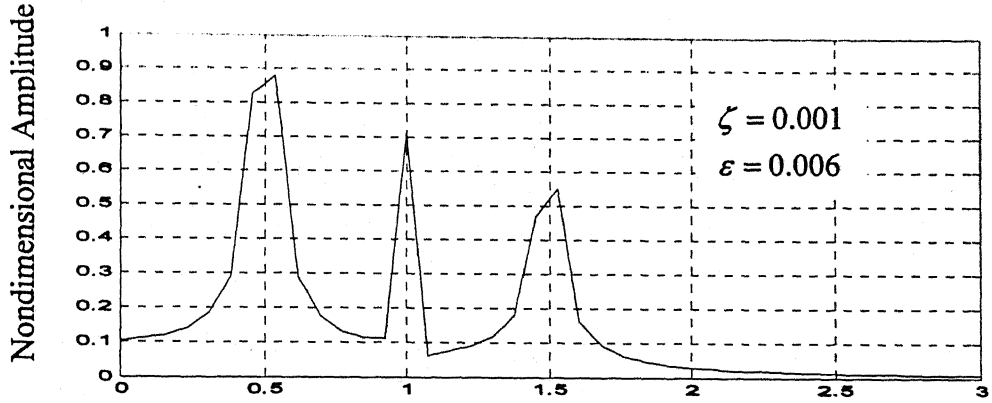

(b) Two tone excitation ($r_1 = 0.5, r_2 = 1.5$)

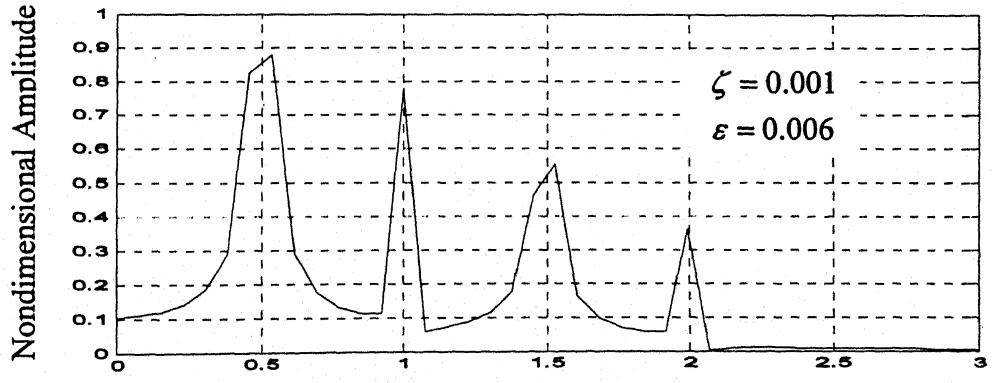

(c) Three tone excitation ($r_1 = 0.5, r_2 = 1.5, r_3 = 2.0$)

Fig. 3.6 Response of a beam with crack
(Crack severity ratio $\varepsilon = 0.006$)

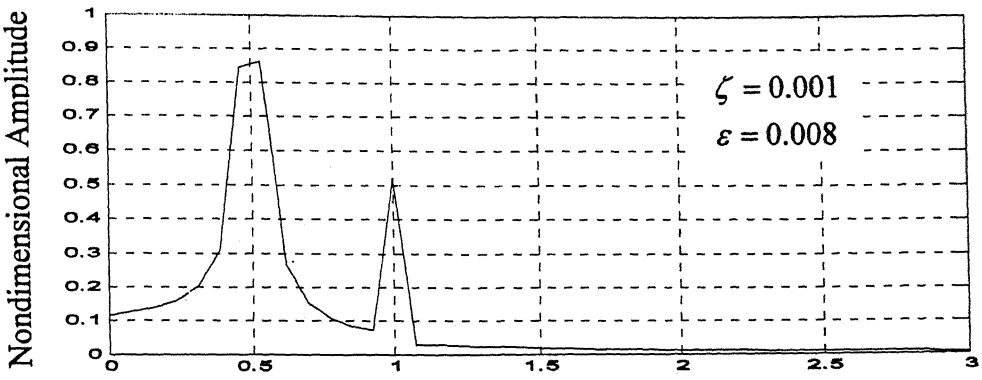

(a) Single tone excitation ($r_1 = 0.5$)

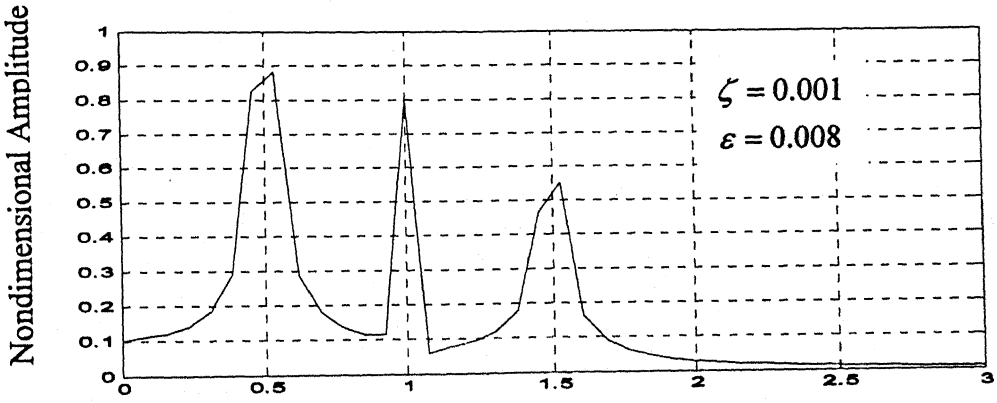

(b) Two tone excitation ($r_1 = 0.5, r_2 = 1.5$)

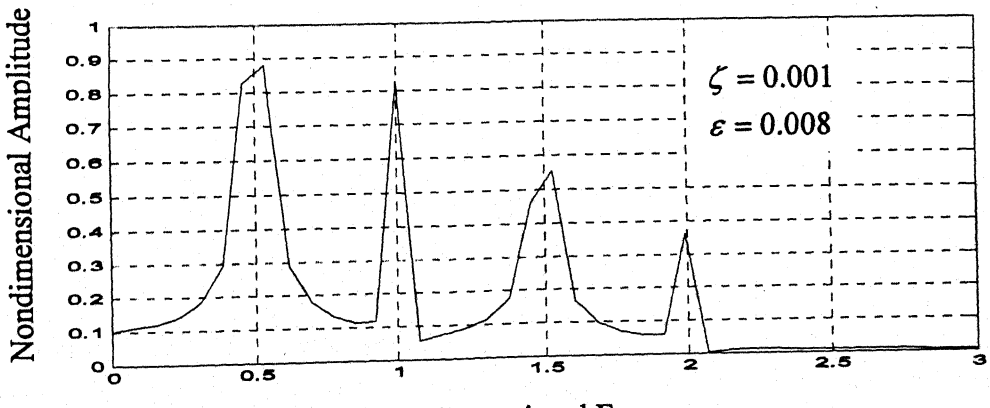

(c) Three tone excitation ($r_1 = 0.5, r_2 = 1.5, r_3 = 2.0$)

Fig. 3.7 Response of a beam with crack
(Crack severity ratio $\varepsilon = 0.008$)

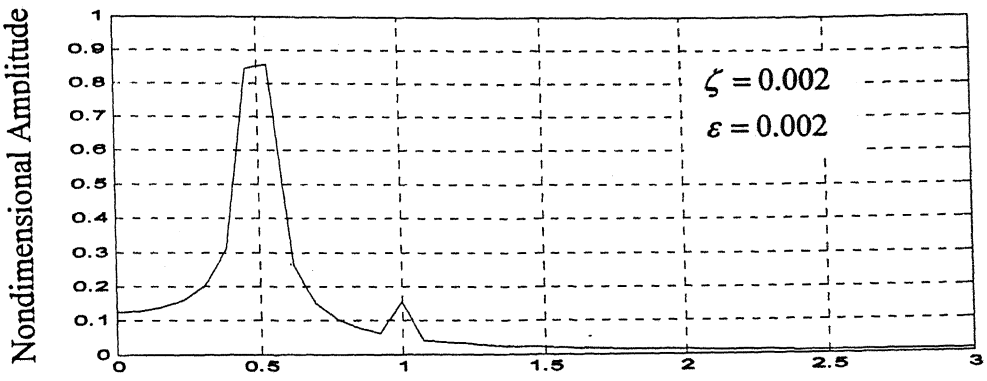

(a) Single tone excitation ($r_1 = 0.5$)

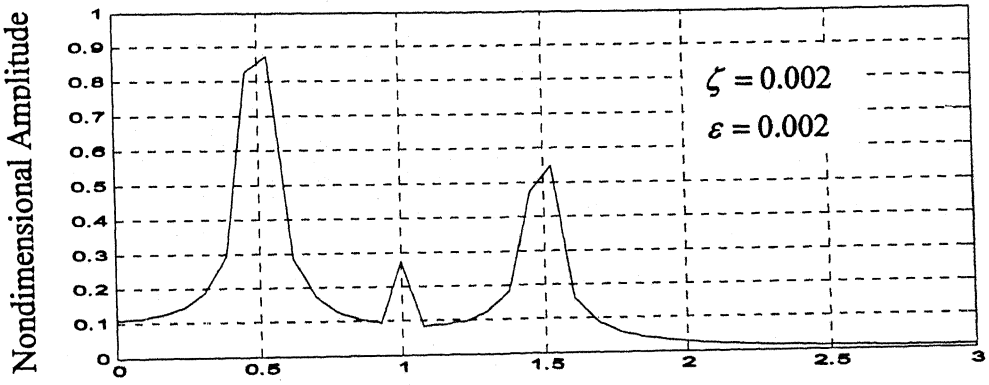

(b) Two tone excitation ($r_1 = 0.5, r_2 = 1.5$)

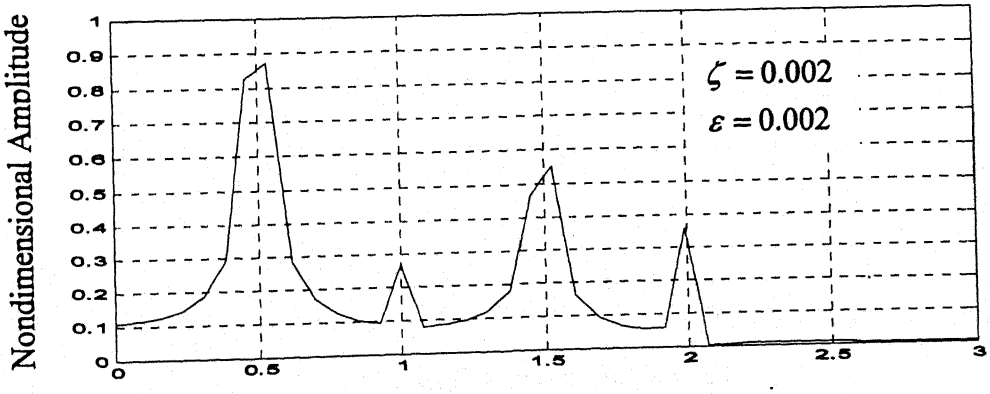

(c) Three tone excitation ($r_1 = 0.5, r_2 = 1.5, r_3 = 2.0$)

Fig. 3.8 Influence of damping on response of beam with crack ($\zeta = 0.002$)

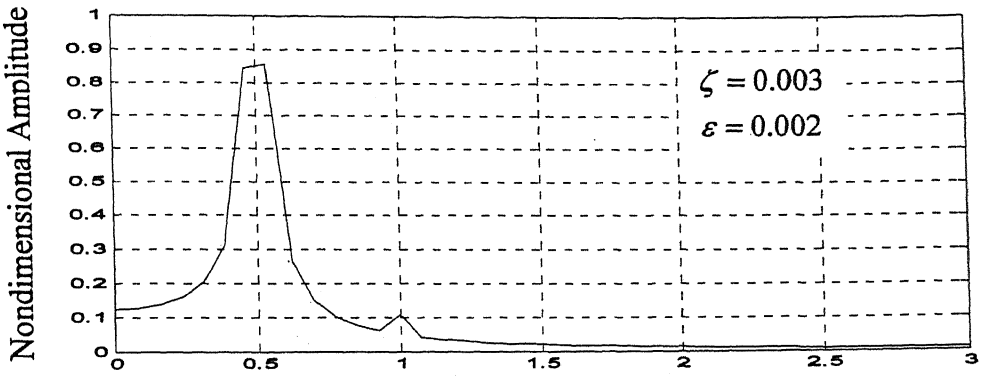

(a) Single tone excitation ($r_1 = 0.5$)

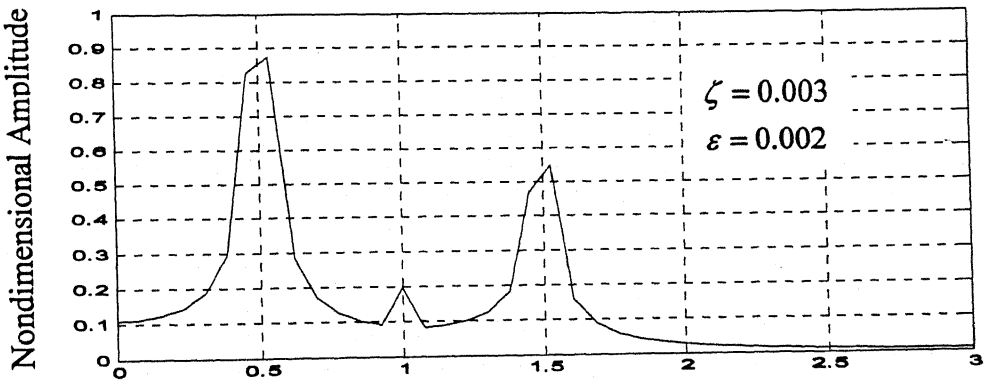

(b) Two tone excitation ($r_1 = 0.5, r_2 = 1.5$)

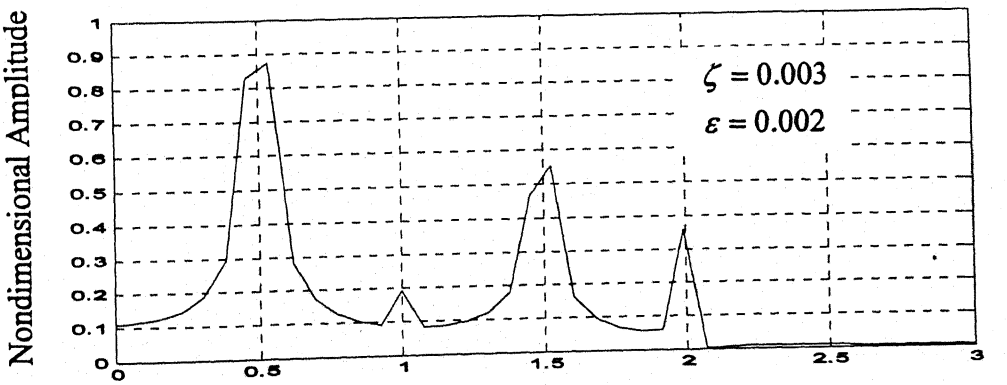

(c) Three tone excitation ($r_1 = 0.5, r_2 = 1.5, r_3 = 2.0$)

Fig. 3.9 Influence of damping on response of beam with crack ($\zeta = 0.003$)

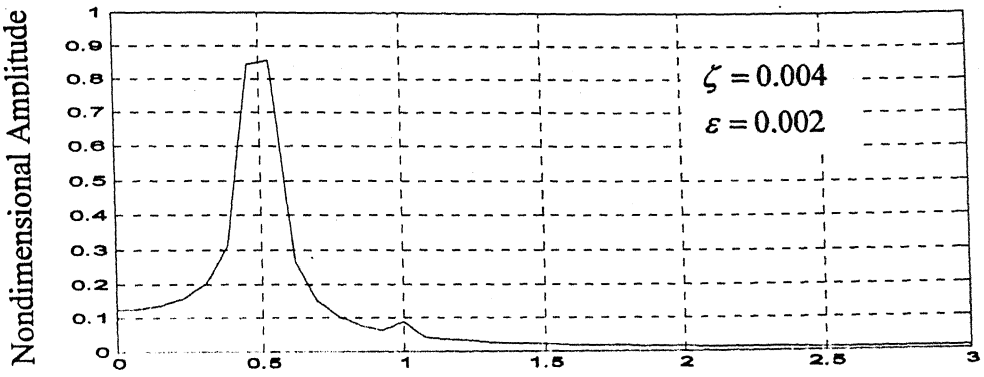

(a) Single tone excitation ($r_1 = 0.5$)

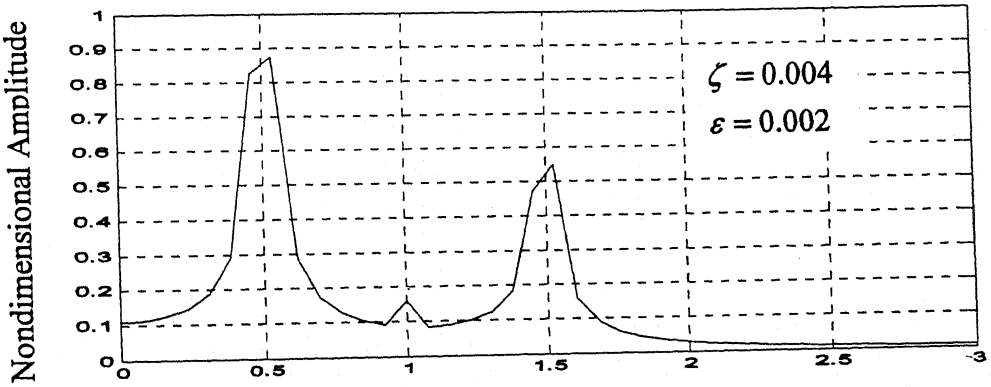

(b) Two tone excitation ($r_1 = 0.5, r_2 = 1.5$)

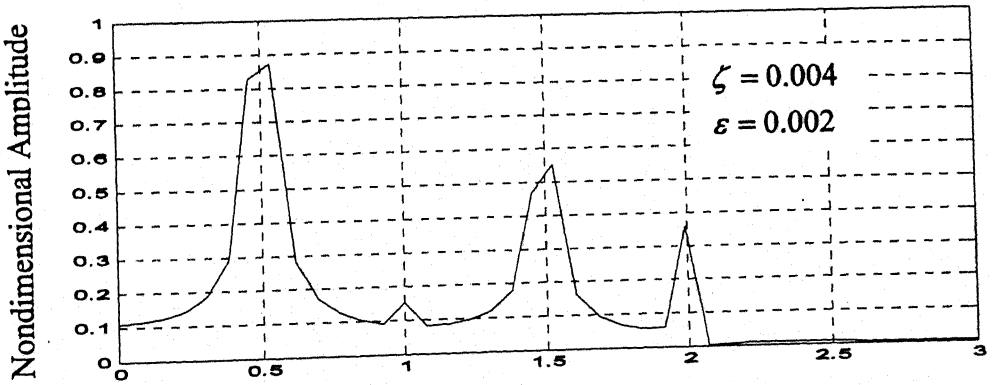

(c) Three tone excitation ($r_1 = 0.5, r_2 = 1.5, r_3 = 2.0$)

Fig. 3.10 Influence of damping on response of beam with crack ($\zeta = 0.004$)

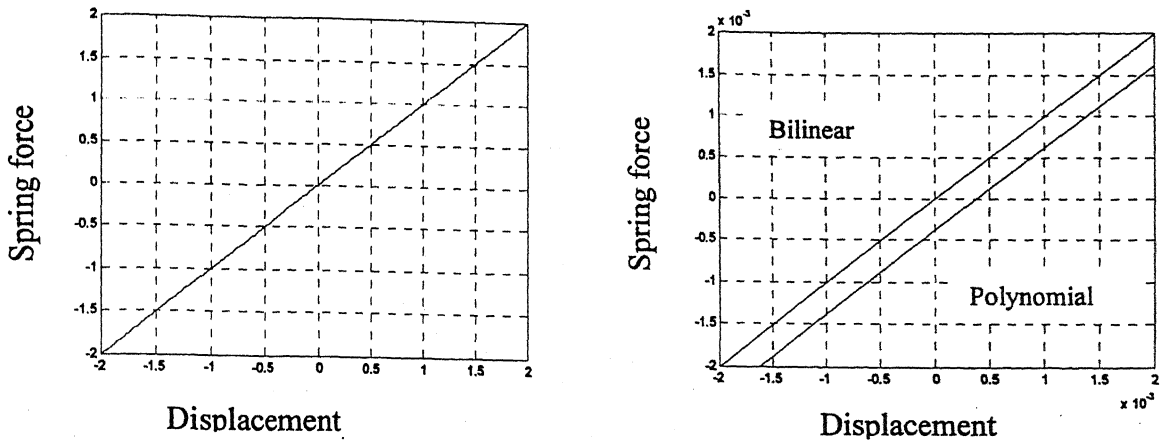

(a) Crack severity ratio $\varepsilon = 0.002$

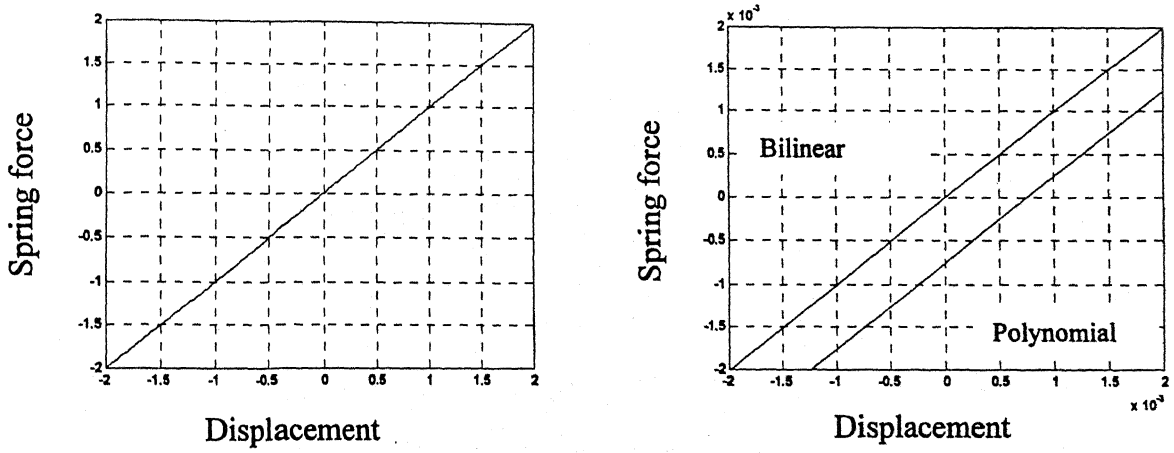

(b) Crack severity ratio $\varepsilon = 0.004$

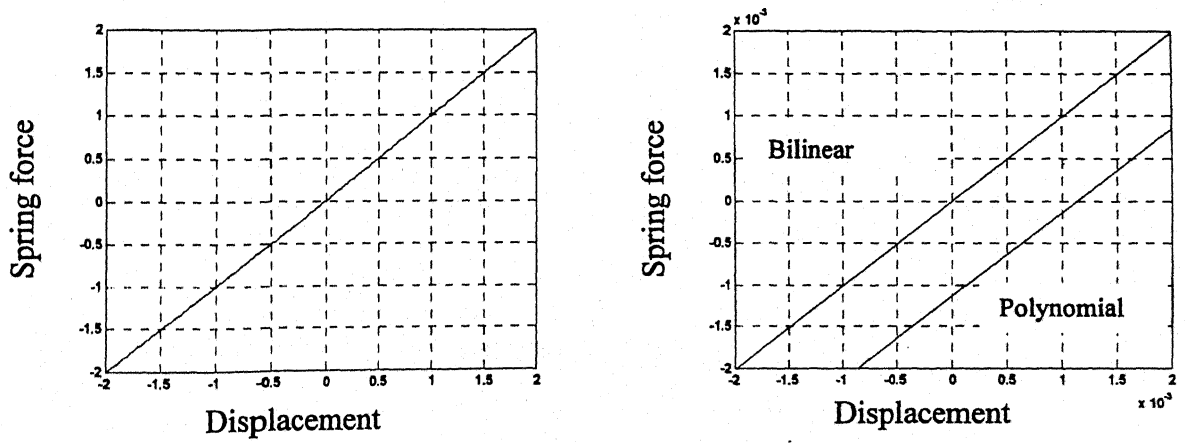

(c) Crack severity ratio $\varepsilon = 0.006$

Fig. 3.11 Comparison of spring forces of bilinear and polynomial models

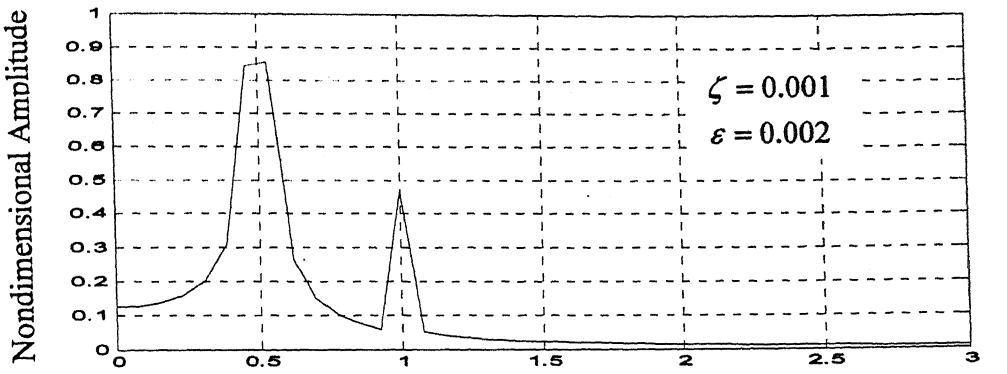

(a) Single tone excitation ($r_1 = 0.5$)

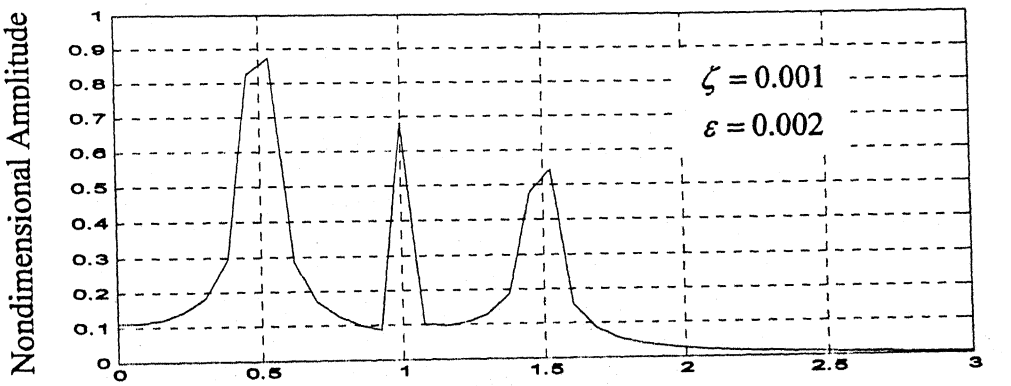

(b) Two tone excitation ($r_1 = 0.5, r_2 = 1.5$)

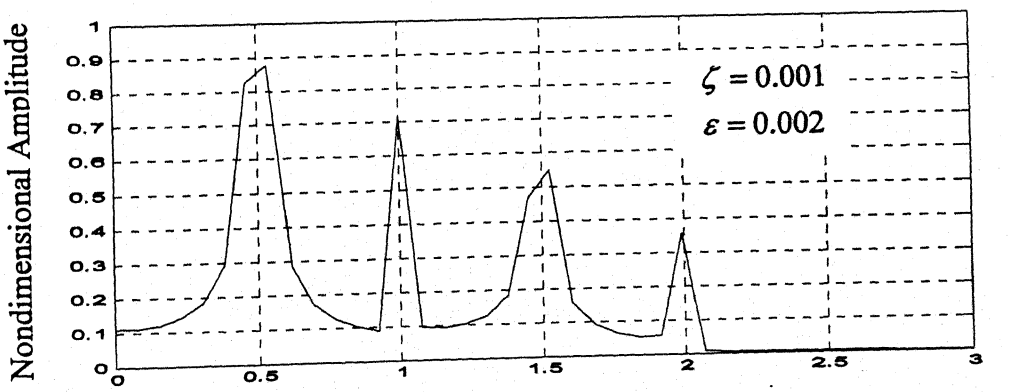

(c) Three tone excitation ($r_1 = 0.5, r_2 = 1.5, r_3 = 2.0$)

Fig. 3.12 Response of equivalent polynomial model ($\varepsilon = 0.002$)

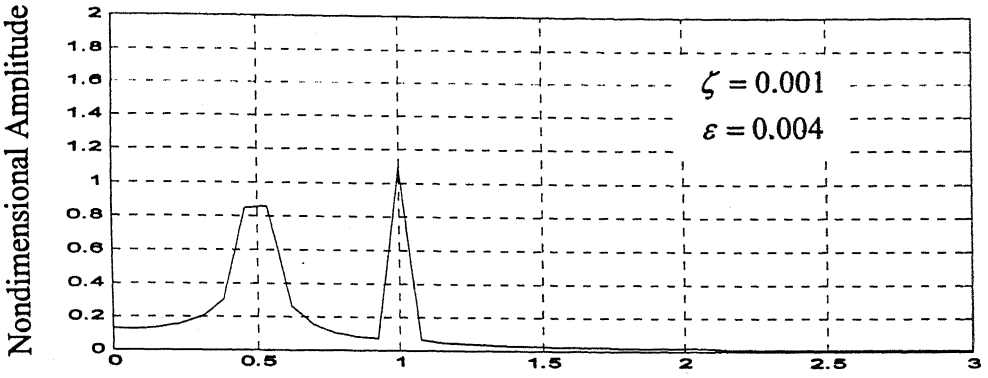

(a) Single tone excitation ($r_1 = 0.5$)

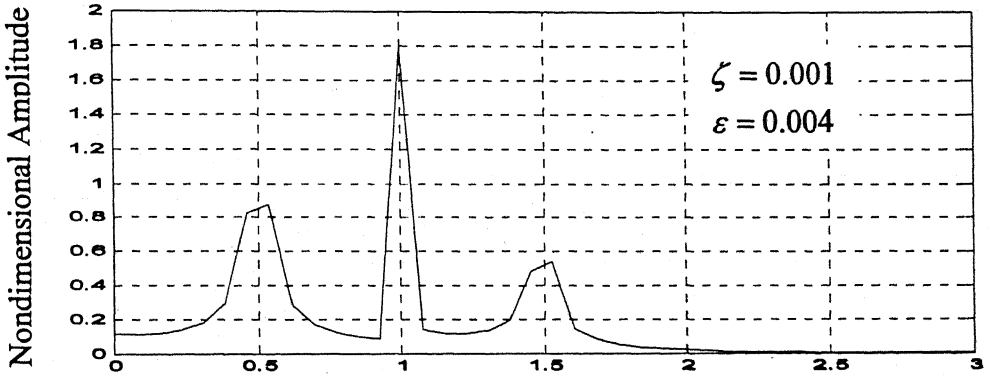

(b) Two tone excitation ($r_1 = 0.5, r_2 = 1.5$)

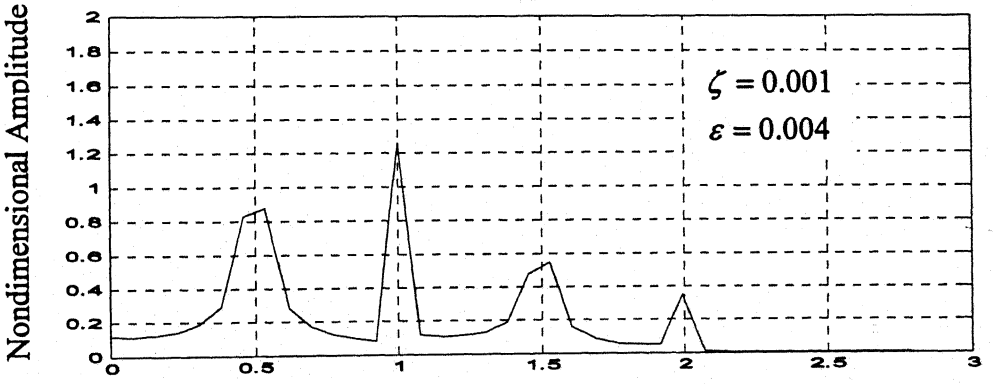

(c) Three tone excitation ($r_1 = 0.5, r_2 = 1.5, r_3 = 2.0$)

Fig. 3.13 Response of equivalent polynomial model ($\varepsilon = 0.004$)

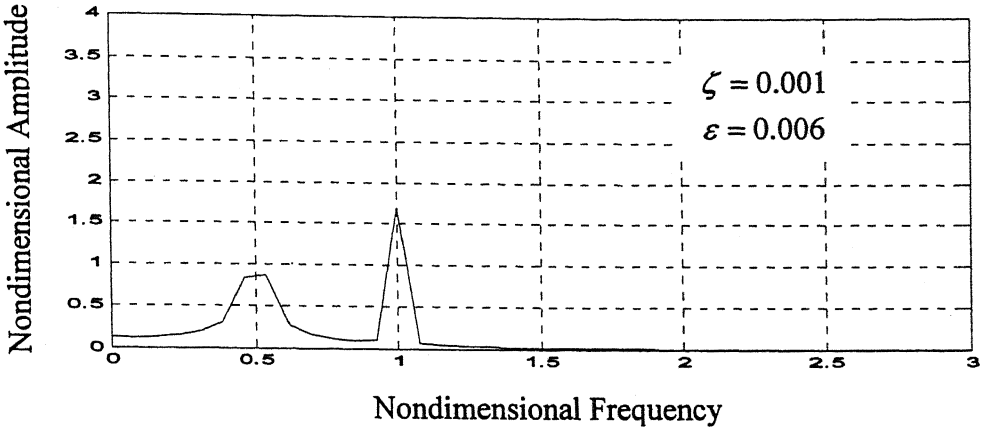

(a) Single tone excitation ($r_1 = 0.5$)

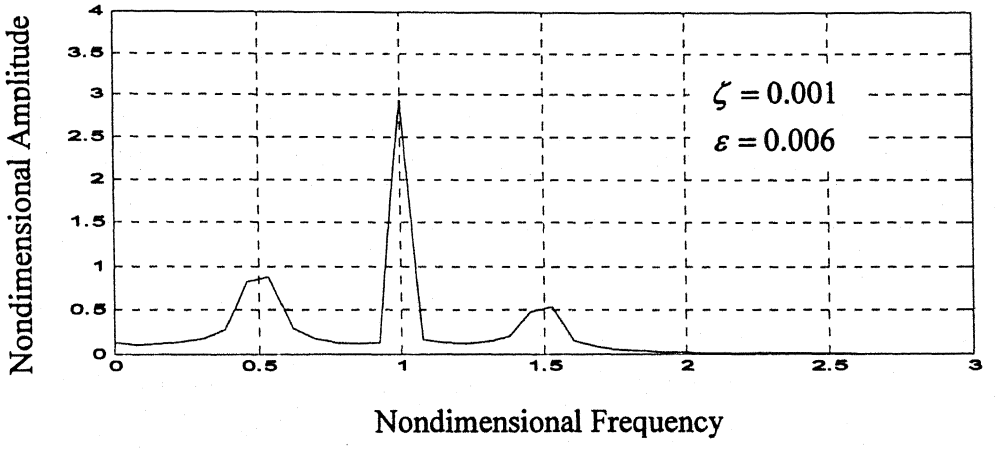

(b) Two tone excitation ($r_1 = 0.5, r_2 = 1.5$)

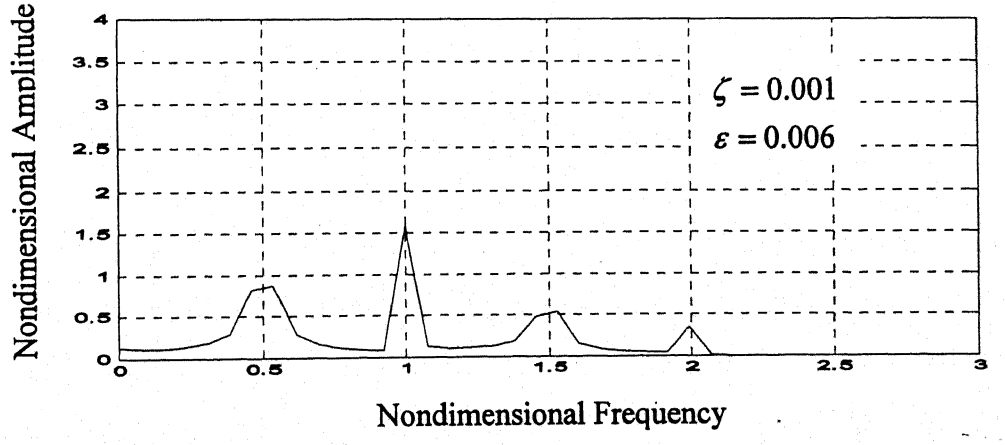

(c) Three tone excitation ($r_1 = 0.5, r_2 = 1.5, r_3 = 2.0$)

Fig. 3.14 Response of equivalent polynomial model ($\varepsilon = 0.006$)

CHAPTER 4

EXPERIMENTAL INVESTIGATIONS

Experimental investigations have been carried out for better understanding of the proposed crack detection procedure. The experiments were carried out on a readily available thin beam. Single tone, two tone and three tone harmonic excitation signals were generated through Virtual Instruments developed in the programming software LabVIEW. Response of the beam was obtained for these forces. A transverse crack was then generated in the same beam and the exercise was repeated to obtain the response for the three types of excitation.

4.1 Experimental Set-Up

The experimental set-up comprised a thin, mild steel beam mounted on an electrodynamic shaker at one end (Fig.4.1). The beam approximately represented a cantilever configuration. Two beams were chosen for experimentation. The geometric and material properties of the beams are given below.

Beam 1:

Length, l=0.170m Width, w=0.01672m Thickness, d=0.00054 m

Modulus of Elasticity, E=200 GPa, Density, $\rho = 8000\, kg/m^3$

Beam 2:

Length, l=0.170m Width, w=0.01644m Thickness, d=0.0009m

Modulus of Elasticity, E=200 GPa, Density, $\rho = 8000\, kg/m^3$

4.2 Instrumentation

The instrumentation employed for the study is shown in Fig. 4.2. The response of the beam was picked up through a miniature accelerometer Type: 4374 Bruel & Kjaer, Charge Sensitivity: 0.153 pc/ms^{-2}, Voltage Sensitivity: 0.197 mv/ms^{-2}. The signal from the accelerometer was conditioned and amplified in a Charge Amplifier (Bruel & Kjaer, Type 2635). The excitation signals for the Electrodynamic Shaker was generated in a Pentium PC, using LabVIEW. LabVIEW is program development application, much like C or BASIC. However, LabVIEW uses graphical programming language, G, to create programs in block diagram form. In addition

of having extensive libraries of functions, LabVIEW includes libraries for data acquisition, GPIB and serial instrument control, data analysis, data presentation, and data storage. The programs developed in LabVIEW are called virtual instruments (VI_s) because their appearance and operation can imitate actual instruments. Thus a *VI* consists of:

Front panel: The interactive user interface of the program is called front panel, because it simulates the panel of a physical instrument. The front panel can contain knobs, push buttons, graphs, and other controls and indicators. Data can be entered using mouse or keyboard.

Block Diagram: The block diagram is a pictorial solution to a programming problem. It is also the source code for the *VI*

The Front Panel and Block Diagram for a typical three tone excitation signal, developed during the course of this study, are shown in Figs. 4.3 (a), (b). The PC is equipped with an A/D card (National Instruments, Texas, AT-MIO-E16, with a scan rate of 250000 samples/s). The signal generated by the VI and coming out through the card is taken through an accessory (BNC 2090), which connects the A/D card to BNC type connectors, to a Power Amplifier (Type: SS250, MB Dynamics, Inc.) The output of the Power amplifier is fed to the electrodynamic shaker. The response signal can also be taken to the computer, through the A/D card. Typical VI for data acquisition and display is shown in Figs. 4.4 (a), (b).

4.3 Experimental Results

Prior to carrying out, crack detection exercise, a Rap-Test was performed on the beam to identify its natural frequency. The beam was very slightly perturbed (to keep the vibrations in the linear zone) at its free end and the resultant free vibrations were recorded. The FFT of this response is shown in Figs. 4.5 (a) and (b), for the two beams. The natural frequency can be seen as

Beam 1: 14 Hz

Beam 2: 22 Hz

The natural frequency were calculated theoretically also, employing the formula

$$\omega_n = (\beta_n l)^2 \sqrt{EI / ml^3}$$

where, for a cantilever configuration $(\beta_1 l)^2 = 3.52$. The theoretical natural frequencies are

Beam 1: 15.13 Hz

Beam 2: 25.21 Hz

The excitation frequencies, in accordance with the procedure described in the earlier chapter, were chosen for Beam 1 as:

Single Tone: $\omega_1 = 7\,\text{Hz}$

Two Tone: $\omega_1 = 7\,\text{Hz}, \omega_2 = 21\,\text{Hz}$

Three Tone: $\omega_1 = 7\,\text{Hz}, \omega_2 = 21\,\text{Hz}, \omega_3 = 28\,\text{Hz}$

These excitation forces, in the time and frequency domain are shown in Figs.4.6-4.8.

The FFT of the response, for the beam without crack, for the three sets of excitation are shown successively in Figs. 4.9 (a)-(c). It can be noticed that the response harmonics pertain to the excitation frequencies, with no combinational harmonics, indicating linearity in the system.

A transverse notch, of 0.2 mm depth, was then made along the width of the beam, at a distance of 127 mm from its free end. This was done by means of a hacksaw, without dismounting the beam from the shaker. A Rap Test was again conducted, in order to detect the natural frequency of the beam after introduction of crack. No noticeable change in natural frequency was observed (from those recorded previously, when there was no crack). The beam was now energised through single tone excitation of Fig. 4.6. The response recorded is shown in Fig. 4.10(a). The presence of a small $2\omega_1 = 14Hz$ peak, in addition to the one at $\omega_1 = 7Hz$, corresponding to the excitation frequency was an indication of nonlinearity in the system, due to introduction of crack. When the two tone excitation of Fig.4.7 was applied, as expected the peak at 14 Hz, was seen to increase in magnitude (Fig.4.10 b). The response to three tone excitation of Fig. 4.8 is given in Fig. 4.10 (c). No significant change seems to be caused in the peak response at 14 Hz, due to the introduction of the third tone in the excitation force. This, as mentioned earlier may be due to the fact that the cubic nature of the nonlinearity may be insignificant in comparison to the square term. However, no attempt was made in the present study to determine the nonlinear parameters.

For Beam 2, the following set of excitation frequencies were chosen.

Single Tone: $\omega_1 = 11\,\text{Hz}$

Two Tone: $\omega_1 = 11\,\text{Hz}, \omega_2 = 33\,\text{Hz}$

Three Tone: $\omega_1 = 11\,\text{Hz}, \omega_2 = 33\,\text{Hz}, \omega_3 = 44\,\text{Hz}$

The amplitude for each of the tones was kept identical and equal to those shown in Fig. 4.6-4.8. FFT of the response, for the beam without crack, for the three sets of excitation are shown in Figs. 4.11 (a)-(c). The response after introduction of a transverse notch, of 0.4 mm depth, at a distance of 130 mm from the free end is shown in Figs.4.12 (a)-(c). The distinction between the response patterns of the uncracked and cracked beam, is not as sharp as in the case of Beam 1. This may be due to an already existing nonlinearity in the beam without crack. Since the linear/nonlinear nature is critically dependent on the magnitude of applied force, and the consequent displacement level, the need to carry out investigations in a better controlled environment was felt.

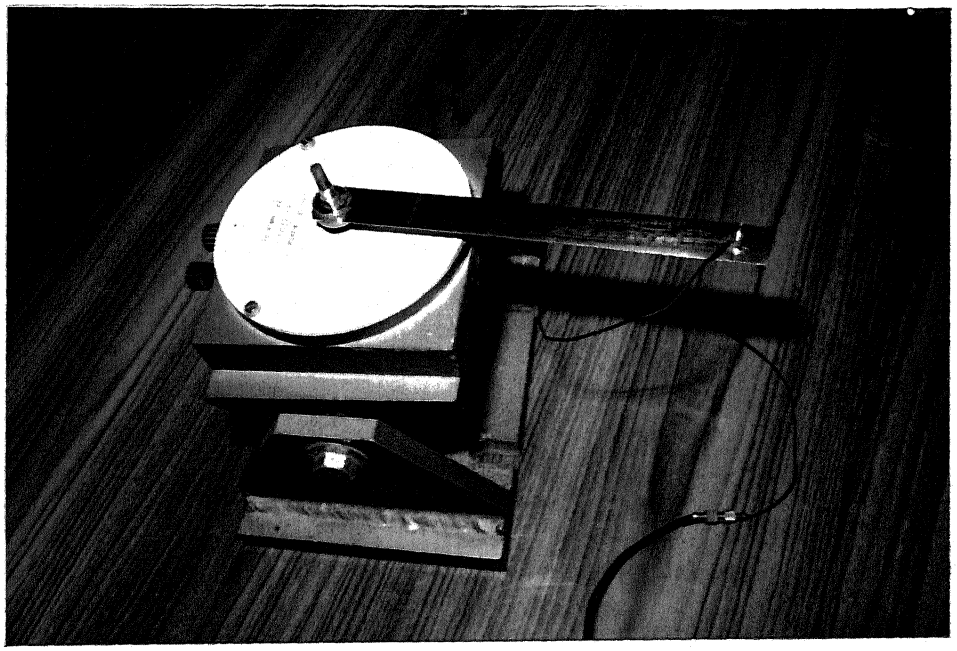

Fig. 4.1 Beam with crack mounted on electrodynamic shaker

Fig. 4.2 Instrumentation

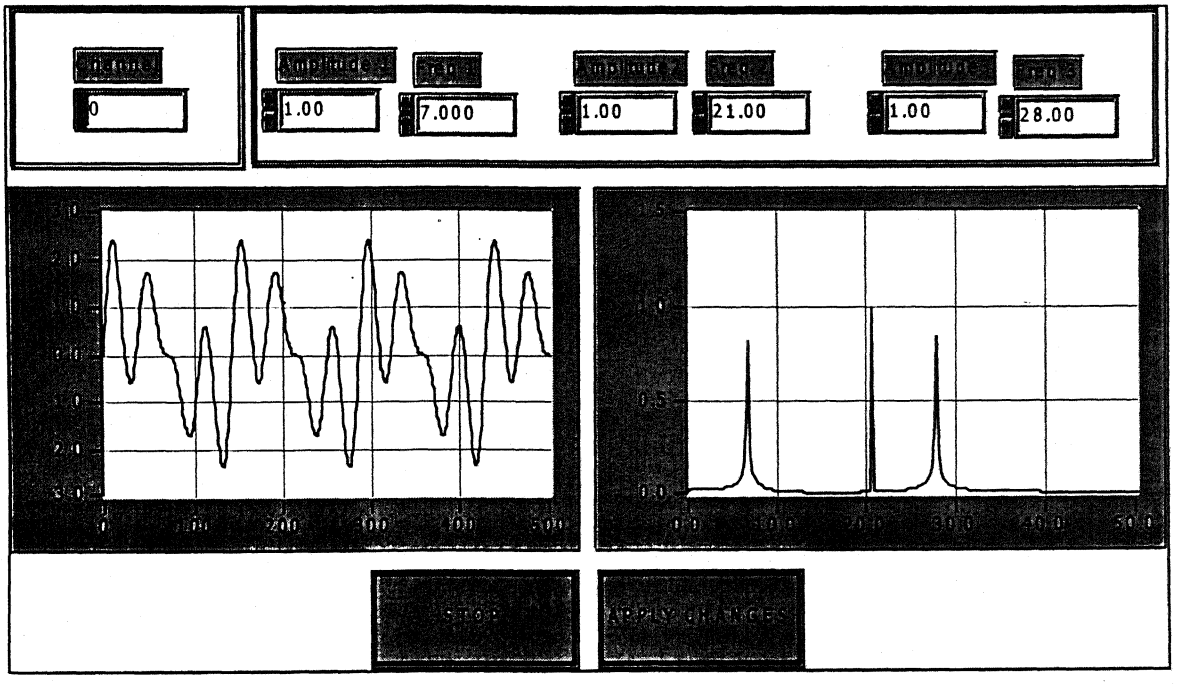

(a) Front panel

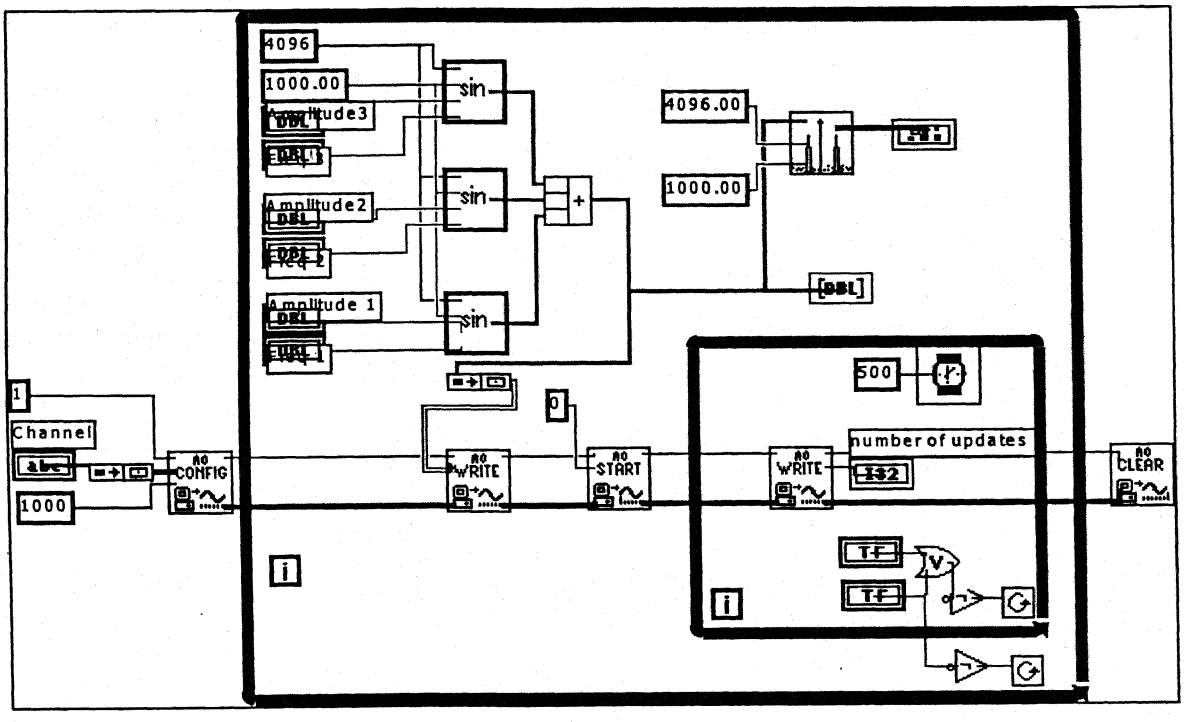

(b) Block Diagram

Fig. 4.3 Description of VI for three tone excitation

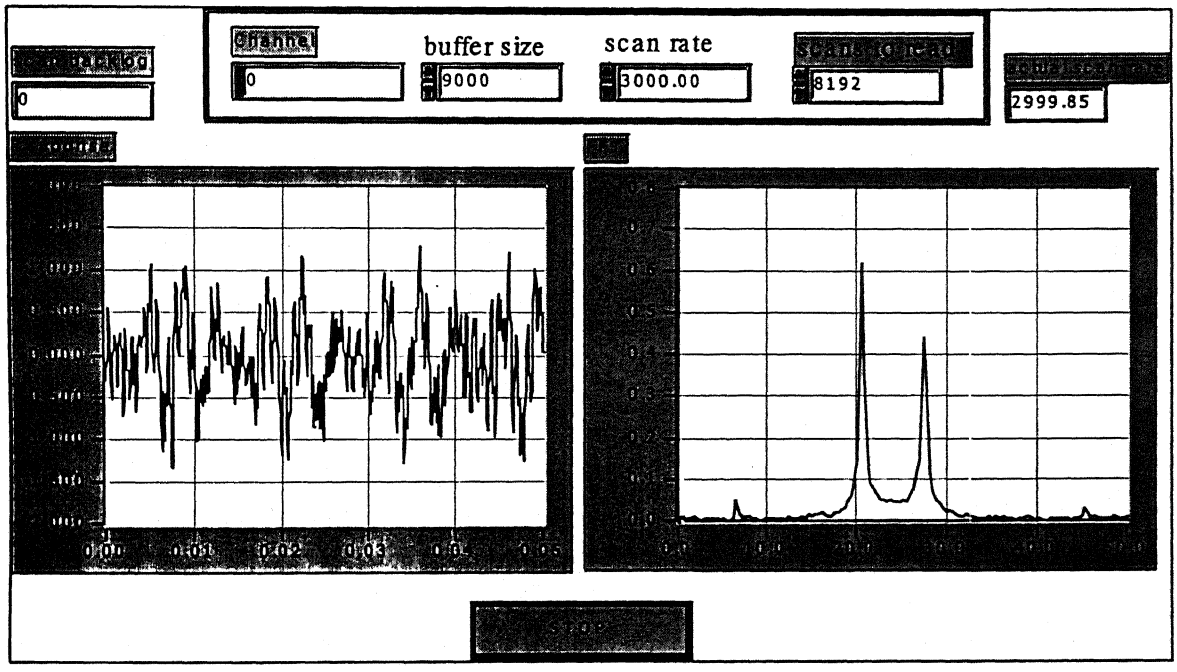

(a) Front panel

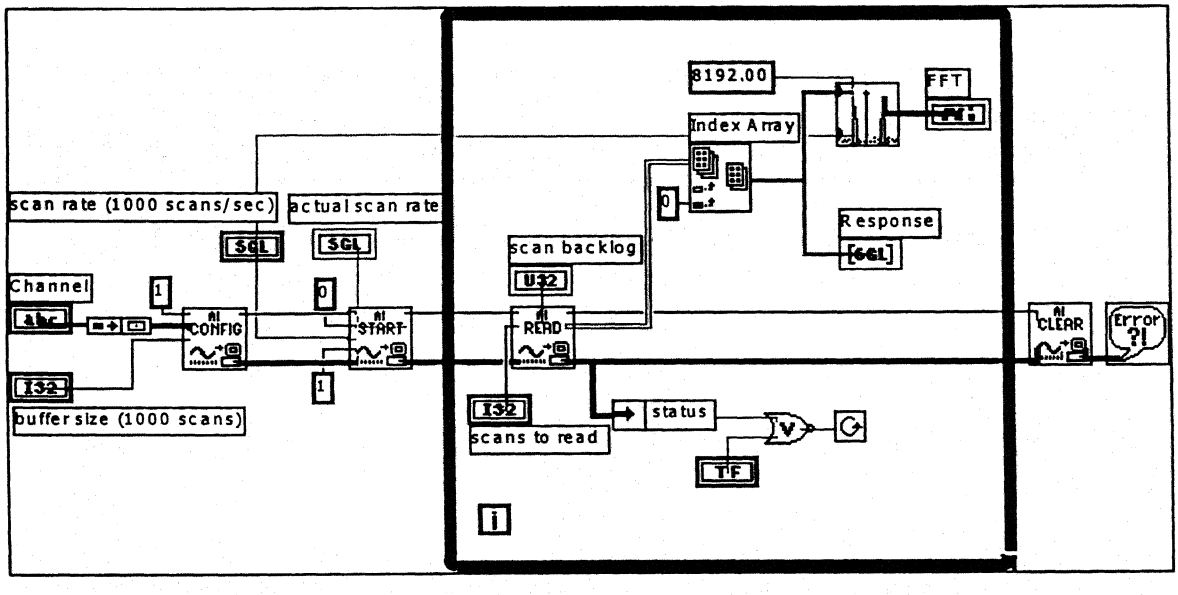

(b) Block Diagram

Fig. 4.4 Description of VI for data acquisition and display

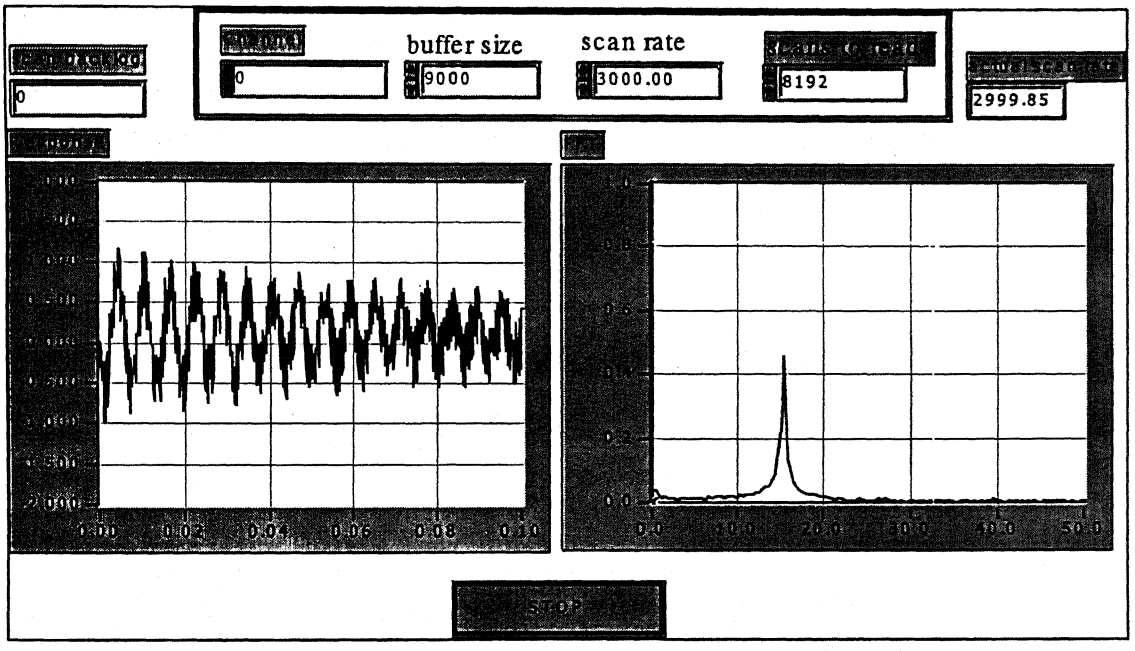

(a) Beam 1

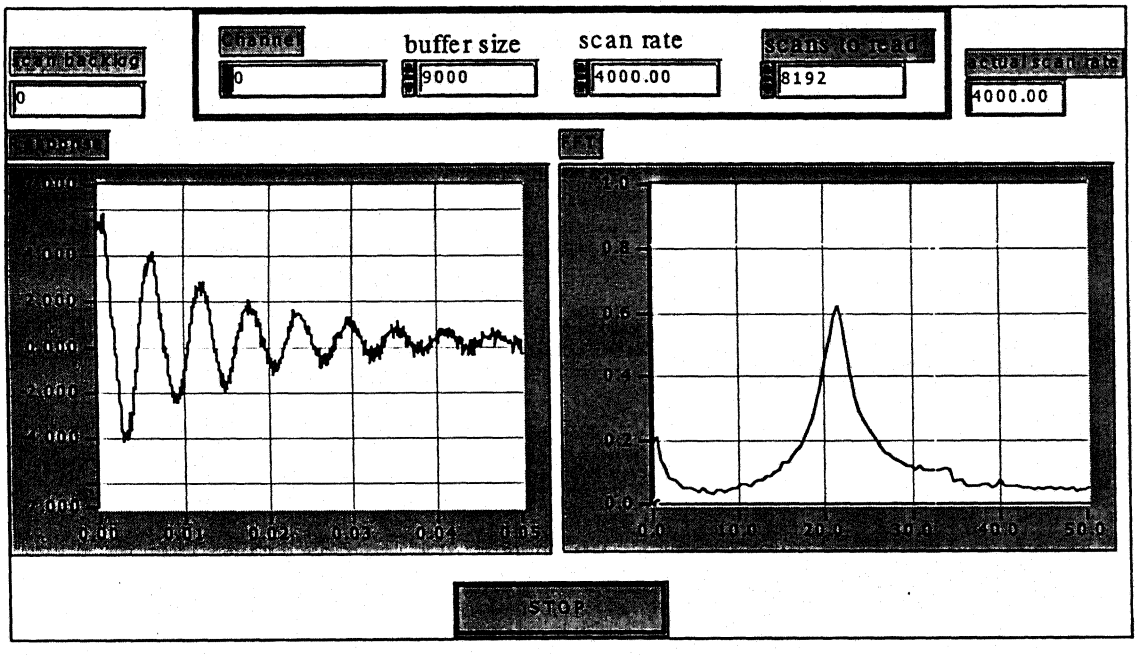

(b) Beam 2

Fig. 4.5 Rap test of beams

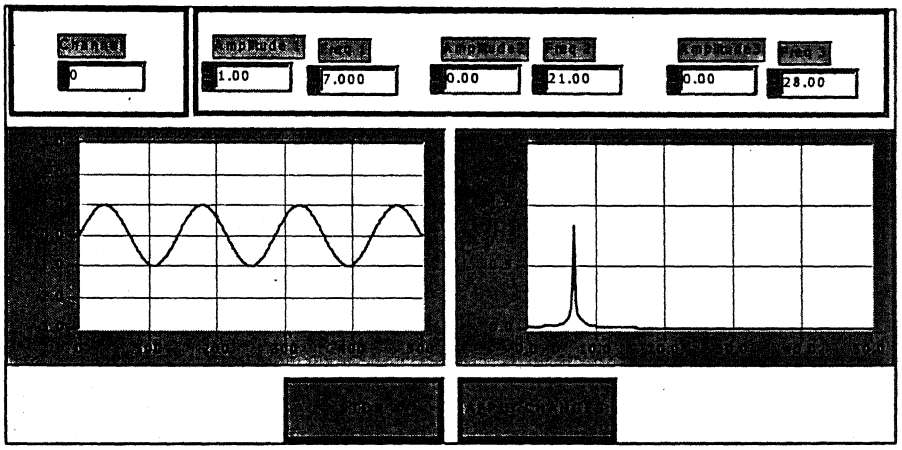

Fig. 4.6 Single tone harmonic excitation for beam 1

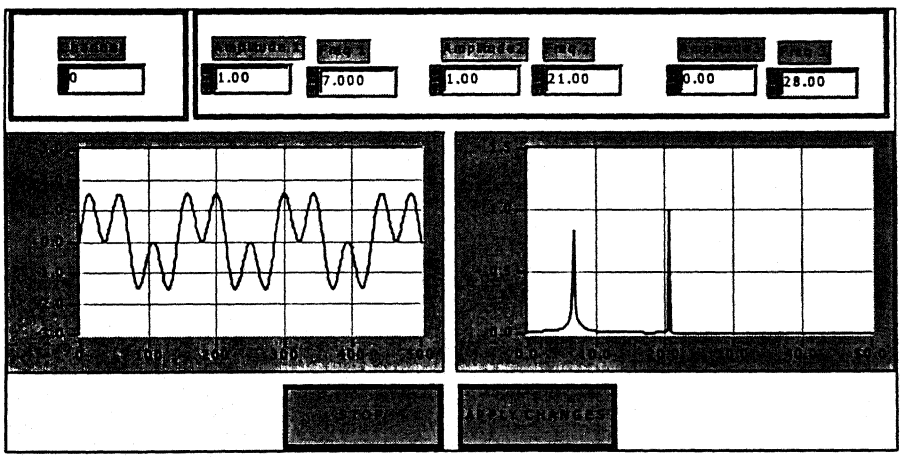

Fig. 4.7 Two tone harmonic excitation for beam 1

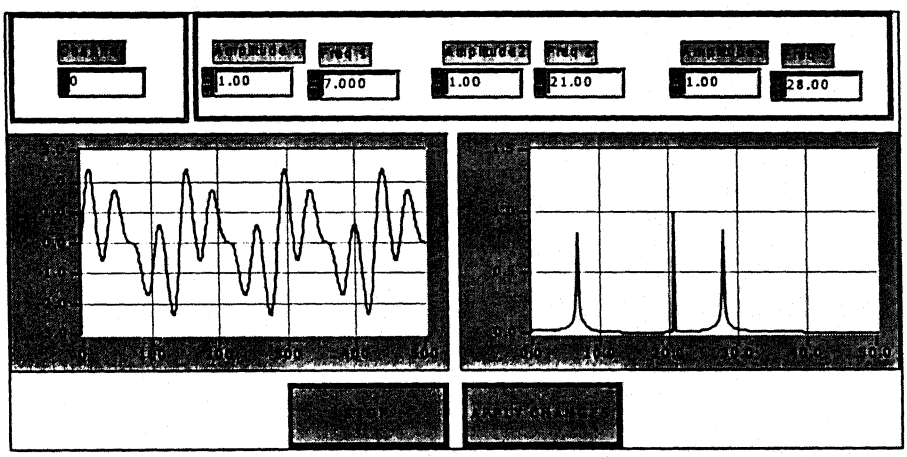

Fig. 4.8 Three tone harmonic excitation for beam 1

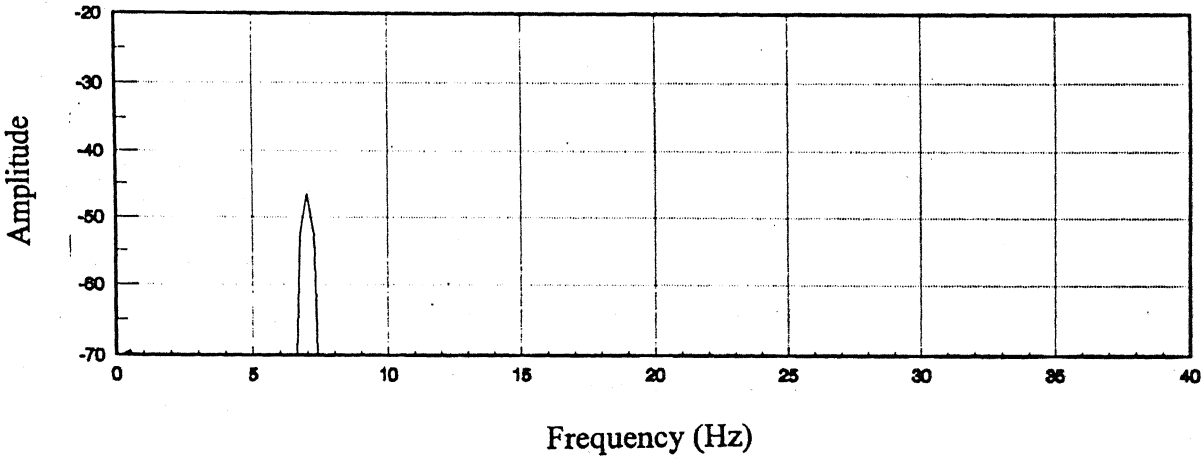

(a) Single tone excitation($\omega_1 = 7Hz$)

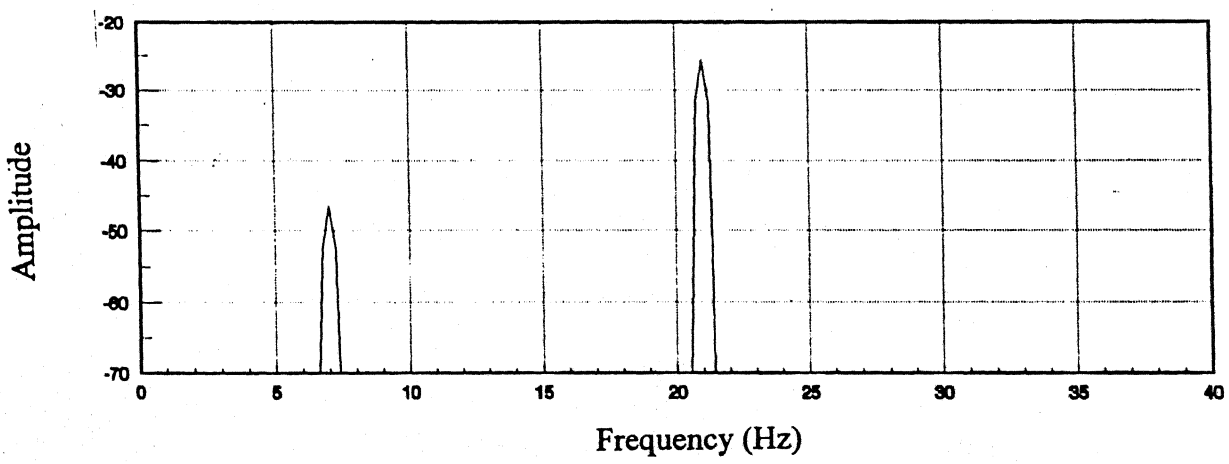

(b) Two tone excitation($\omega_1 = 7Hz, \omega_2 = 21Hz$)

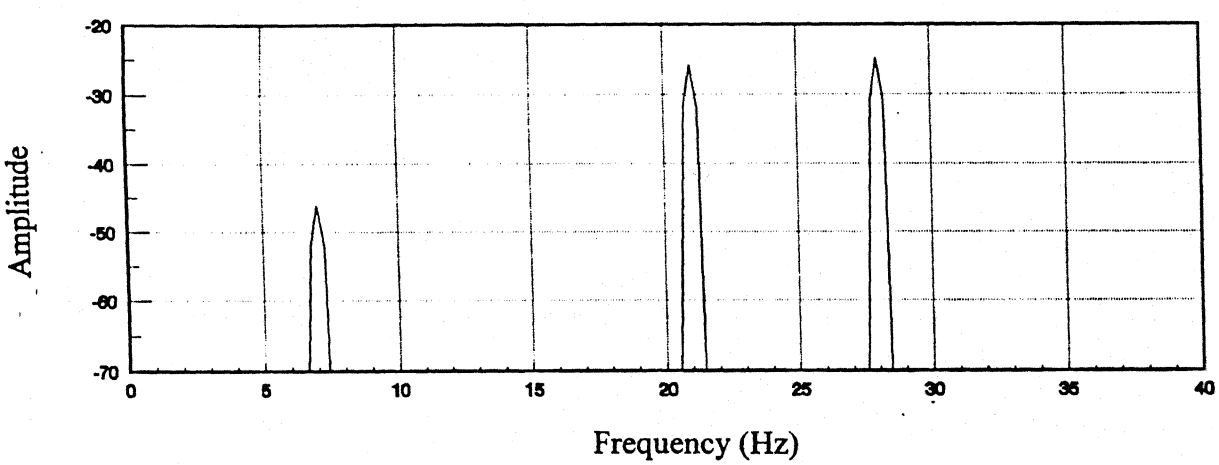

(c) Three tone excitation($\omega_1 = 7Hz, \omega_2 = 21Hz, \omega_3 = 28Hz$)

Fig. 4.9 Response of beam 1 without crack

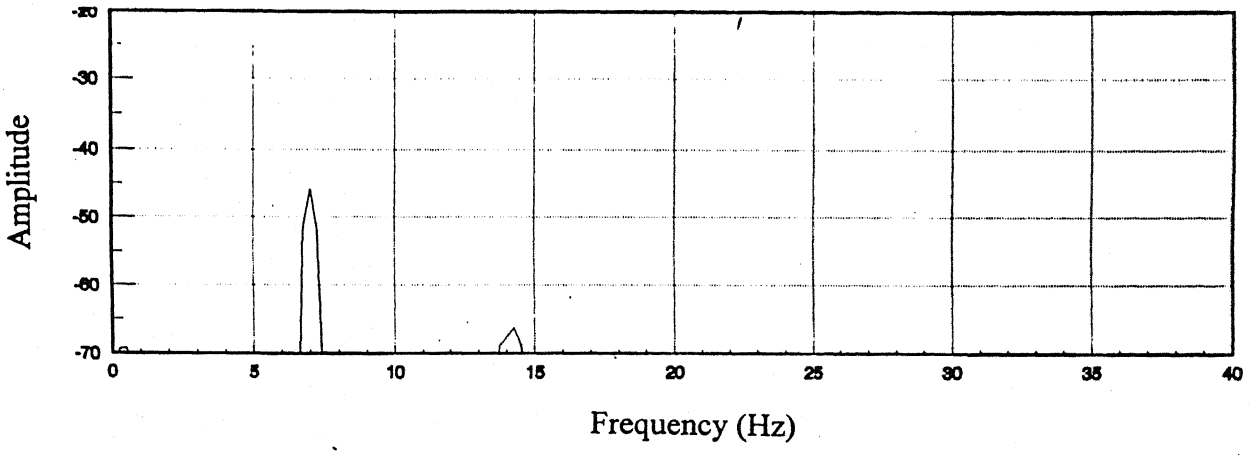

(a) Single tone excitation($\omega_1 = 7Hz$)

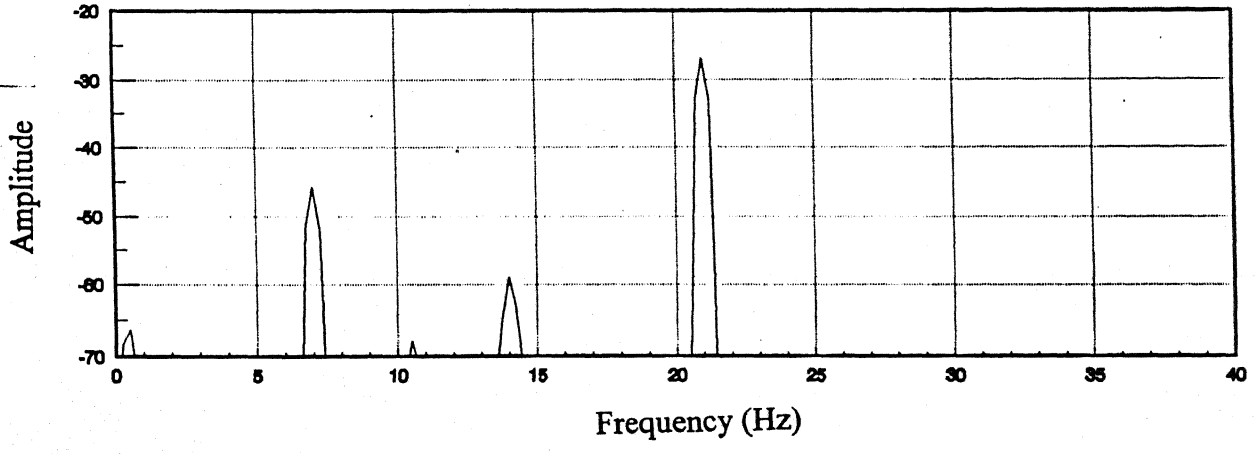

(b) Two tone excitation($\omega_1 = 7Hz, \omega_2 = 21Hz$)

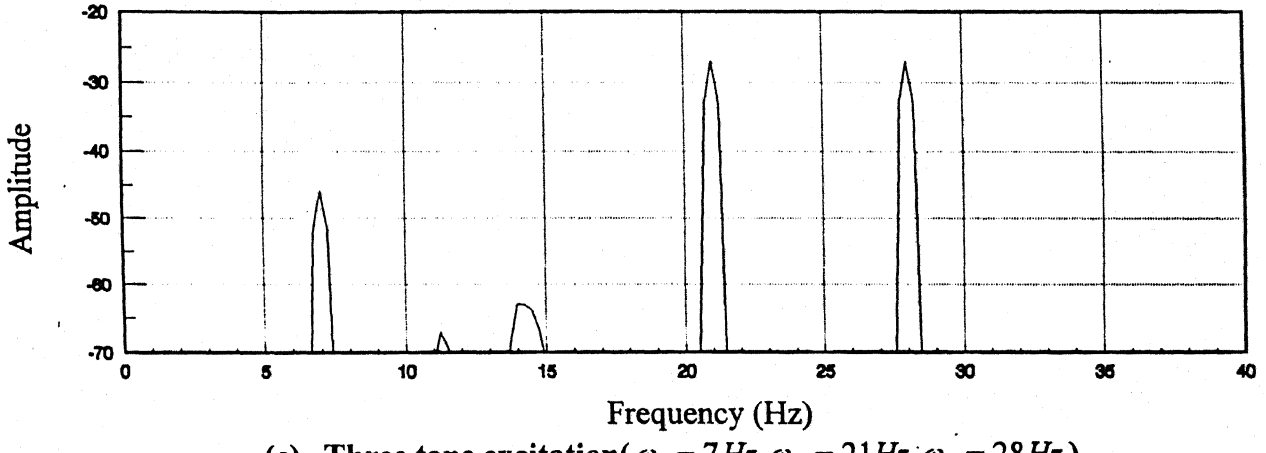

(c) Three tone excitation($\omega_1 = 7Hz, \omega_2 = 21Hz, \omega_3 = 28Hz$)

Fig. 4.10 Response of beam 1 with crack

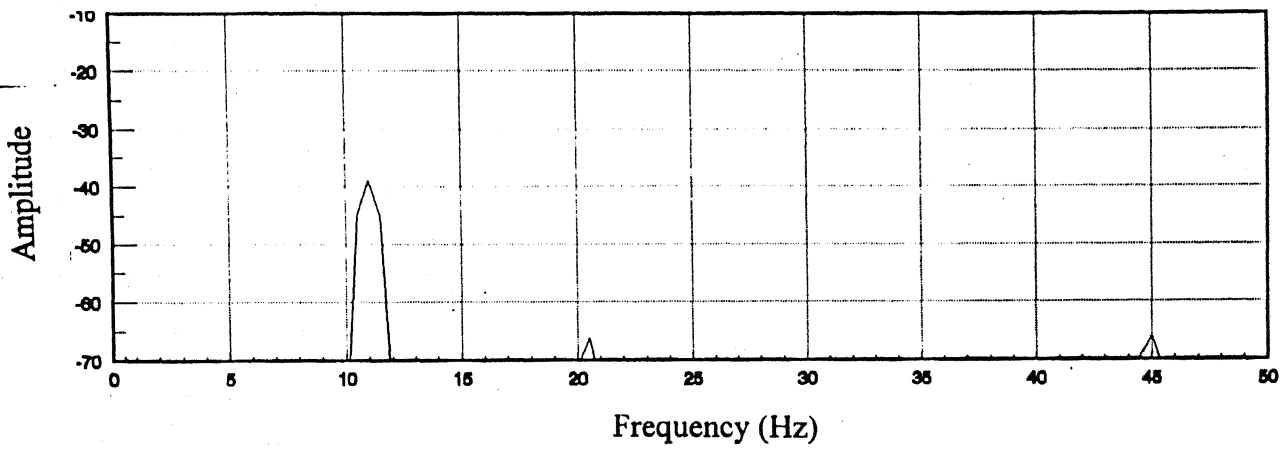

(a) Single tone excitation($\omega_1 = 11Hz$)

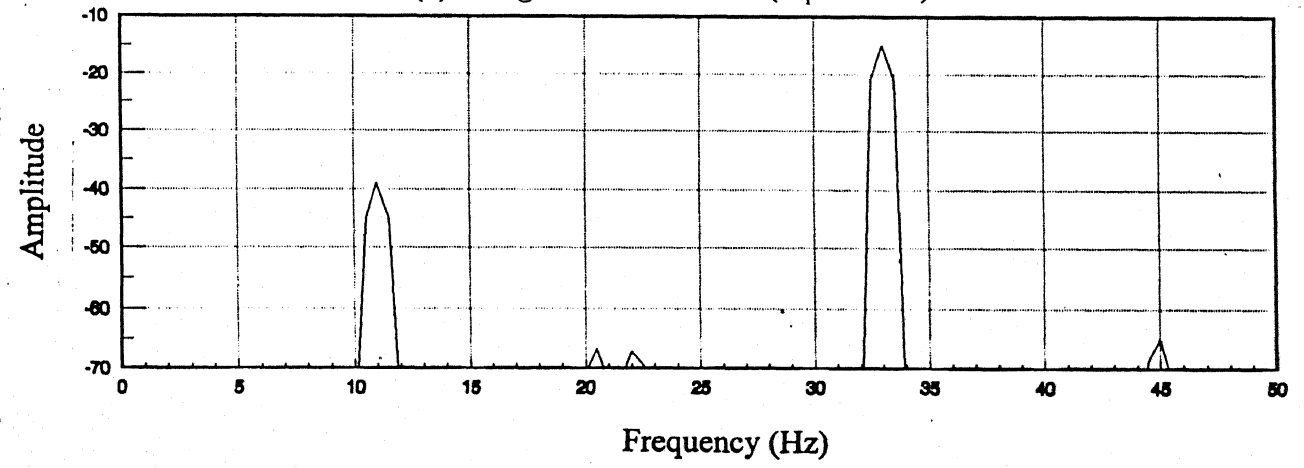

(b) Two tone excitation($\omega_1 = 11Hz, \omega_2 = 33Hz$)

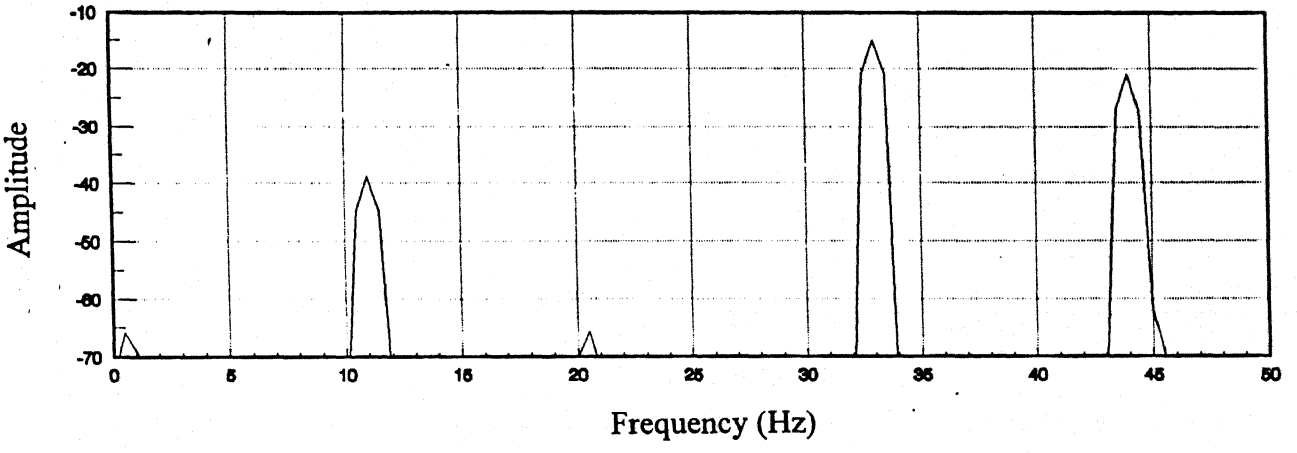

(c) Three tone excitation($\omega_1 = 11Hz, \omega_2 = 33Hz, \omega_3 = 44Hz$)

Fig. 4.11 Response of beam 2 without crack

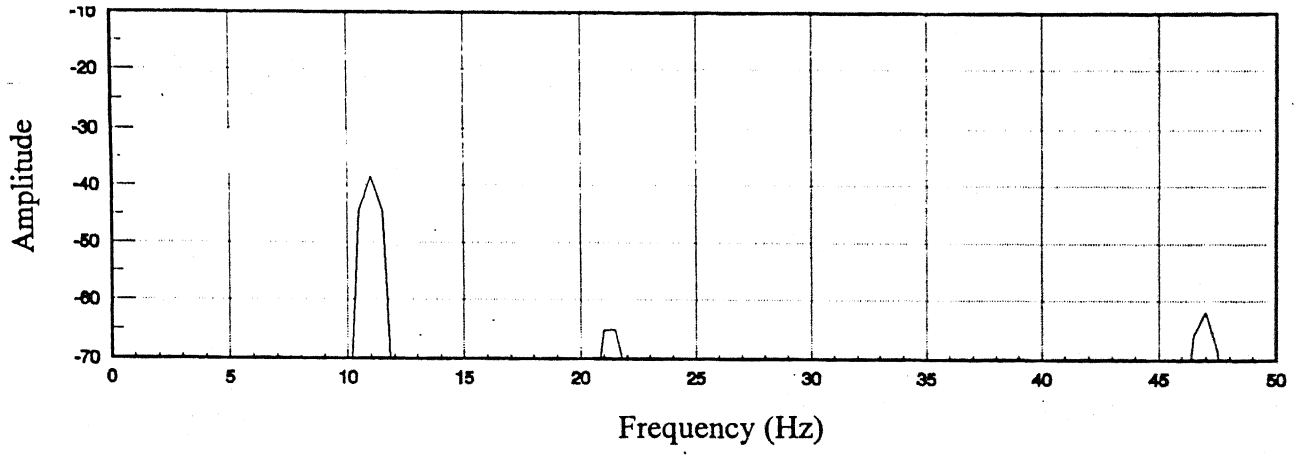

(a) Single tone excitation($\omega_1 = 11Hz$)

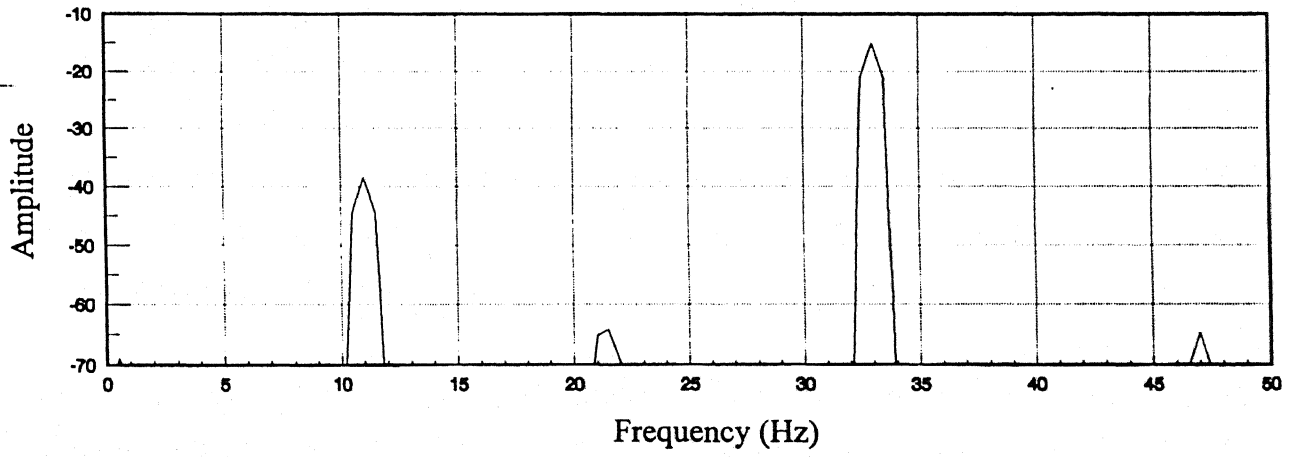

(b) Two tone excitation($\omega_1 = 11Hz, \omega_2 = 33Hz$)

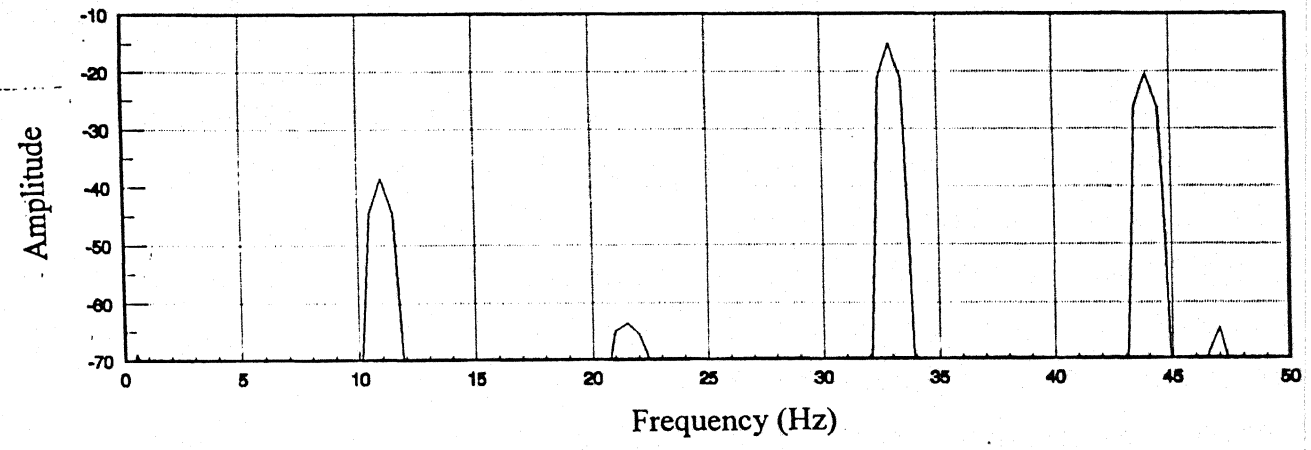

(c) Three tone excitation($\omega_1 = 11Hz, \omega_2 = 33Hz, \omega_3 = 44Hz$)

Fig. 4.12 Response of beam 2 with crack

CHAPTER 5

CONCLUSIONS

The modeling, numerical simulation and experimentation carried out in this study, suggest that multi tone harmonic excitation and higher order FRF analysis can be developed as effective tools for transverse crack detection in beams. Bilinear and equivalent polynomial models can account for the change in the beam characteristics due to development of a breathing crack, in an effective manner. The numerical simulations carried out, also indicate that fairly small bilinearity in a system can be detected and magnified through multi tone harmonic excitation. In absence of analytical solutions, for a bilinear system, equivalent polynomial models can be built in order to rationalise the response patterns. The equivalent polynomial model also helped to outline a step-by-step procedure for crack detection.

The experimental work confirmed the numerically simulated patterns. The present work also emphasises the utility of Virtual Instrumentation techniques. A multi-tone excitation force could be readily developed in LabVIEW. This would not have been possible through conventional means and three electromagnetic shakers with three signal generators would have been required.

The notch sizes in the experimental beams were, however large, which made crack detection possible. The procedure developed can be useful, if small cracks can be detected. There is a need to carry out experiments in a more controlled environment. The excitation force needs to be carefully controlled. It may be difficult to detect cracks through small excitation forces. Usage of higher excitation force levels may however, force beams without crack also, to vibrate in a nonlinear regime. Presence of crack may then have to be detected, through comparison of two sets of nonlinear response patterns. Experimental work also, needs to be augmented by locating the notch at various points along the length of the beam, in addition to varying its size.

It may be broadly concluded that the technique presented in this thesis, does provide sufficient reasons for its further exploration as a tool for crack detection.

REFERENCES

1. Abraham O.N.L. and Brandon J.A. 1995 Journal of Vibration and Acoustics 17, 370-377. The modelling of the opening and the closure of a crack.
2. Anifantis N., Rizos P.F. and Dimarogonas A.D. American Society of Mechanical Engineers Design Division Publication DE 7, 189-197. Identification of cracks on beams by vibration analysis.
3. Cawley P. and Adams R.D., 1979, Journal of Strain Analysis 14, 49-57. The location of defects in structures from measurements of natural frequencies.
4. Chatterjee A. and Vyas N.S. 1999 Journal of Sound and Vibration (Accepted for publication). Convergence analysis of Volterra series response of nonlinear systems subjected to harmonic excitation.
5. Choi Y.S. and Noah S.T. 1988 Journal of Sound and Vibration 121, 117-126. Forced periodic vibration of unsymmetric piecewise-linear systems.
6. Christides S. and Barr A. 1984 International journal of Mechanical Sciences 26 (11), 639-648, One dimensional theory of cracked Bernoulli-Euler beams.
7. Dimarogonas A.D. and Papadopoulos C.A. 1983, Journal of Sound and Vibration 91, 583-593. Vibration of cracked shaft in bending.
8. Friswell M.I. and Penny J.E.T. 1992 Proceedings of X International Modal Analysis Conference, San Diego, CA1,516-521. A simple non-linear model of a cracked beam.
9. Gounaris G. and Dinarogonas A.D. 1988 Computers & Structures 28, 309-313. A finite element of a cracked prismatic beam for structural analysis.
10. Gudmunson P. 1982 Journal of Mechanics and Physics of Solids 30, 339-353, Eigen frequency changes of structures due to cracks. Notches or other geometrical changes.
11. Gudmunson P. 1983 Journal of Mechanics and Physics of Solids 31, 329-345. The dynamic behavior of slender structures with cross-sectional cracks.
12. Ibrahim A., Ismail F. and Maltin H.R., 1987, Journal of Analytical, Experimental Modal Analysis 2, 76-82. Modelling of the dynamics of continuous beam including non-linear fatigue crack.

13. Krawczuk M. and Ostachowicz W. 1994 Proceedings of ISMA 19, Leuven, Belzium 3, 1067-1078. Forced vibration of a cantilever Timoshanko beam with a closing crack.
14. Nandwana B.P. and Maiti S.K. 1997 Journal of Sound and Vibration 203,435-446. Detection of the location and size of a crack in stepped cantilever beams based on measurements of natural frequency.
15. Ostachowicz W.M. and Krawczuk M. 1991 Journal of Sound and Vibration 150, 191-201. Analysis of the effect of the cracks on the natural frequencies of a cantilever beam.
16. Pandey A.K., Biswas M. and Samman M.M. 1991 Journal of Sound and Vibration 145, 321-332. Damage detection from changes in curvature modal shapes.
17. Qian G.L., Gu S.N. and Jiang J.S. 1990 Journal of Sound and Vibration 138, 232-243. The dynamic behaviour and crack detection of a beam with crack.
18. Rajab M.D. and Al-Sabeeh A. 1991 Journal of Sound and Vibration 147, 465-473. Vibrational characteristics of cracked shafts.
19. Rivola A. and White P.R. 1998 Journal of Sound and Vibration 216, 889-910. Bispectral analysis of the bilinear oscillator with applications to the detection of fatigue cracks.
20. Rizos P.F. and Dimarogonas A.D. 1989 Journal of Sound and Vibration 138, 381-388. Identification of crack location and magnitude in a cantilever beam from the vibration modes.
21. Schetzen M. 1980 The Volterra and Wiener Theories of Nonlinear Systems, John Wiley and Sons, New York.
22. Shen M.H.H. and Chu Y.C 1992 Computers and Structures 45, 79-93. Vibrations of beams with a fatigue crack.
23. Sundermeyer J.N. and Weaver R.L. 1995 Journal of Sound and Vibration 183, 857-871. On crack identification and characterization in a beam by non-linear vibration analysis.
24. Tsai T.C. and Wang Y.Z. 1996 Journal of Sound and Vibration 192, 607-620. Vibration analysis and diagnosis of a cracked shaft.

APPENDIX 1

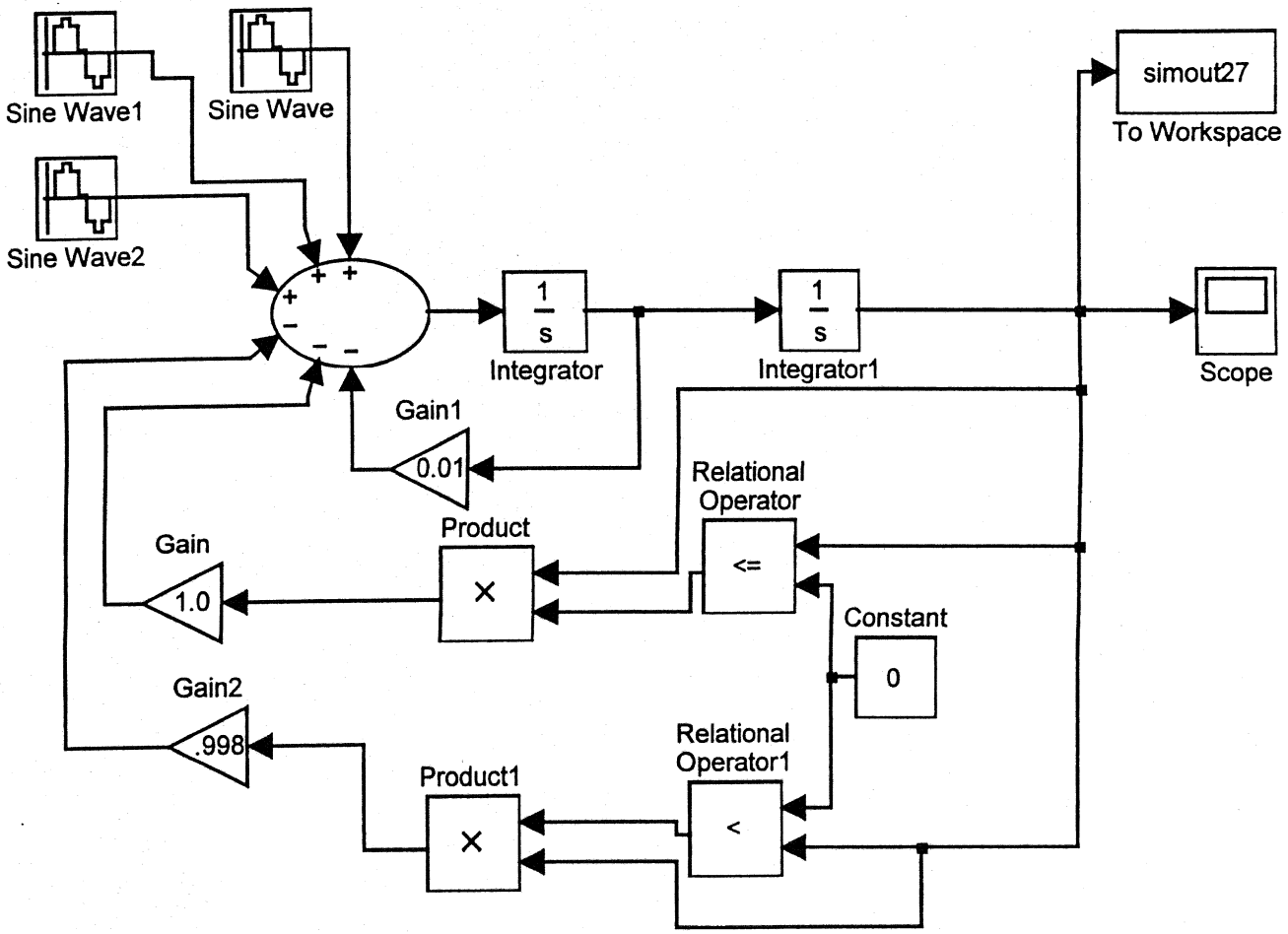

SIMULINK MODEL FOR BILINEAR MODEL RESPONSE

APPENDIX 2

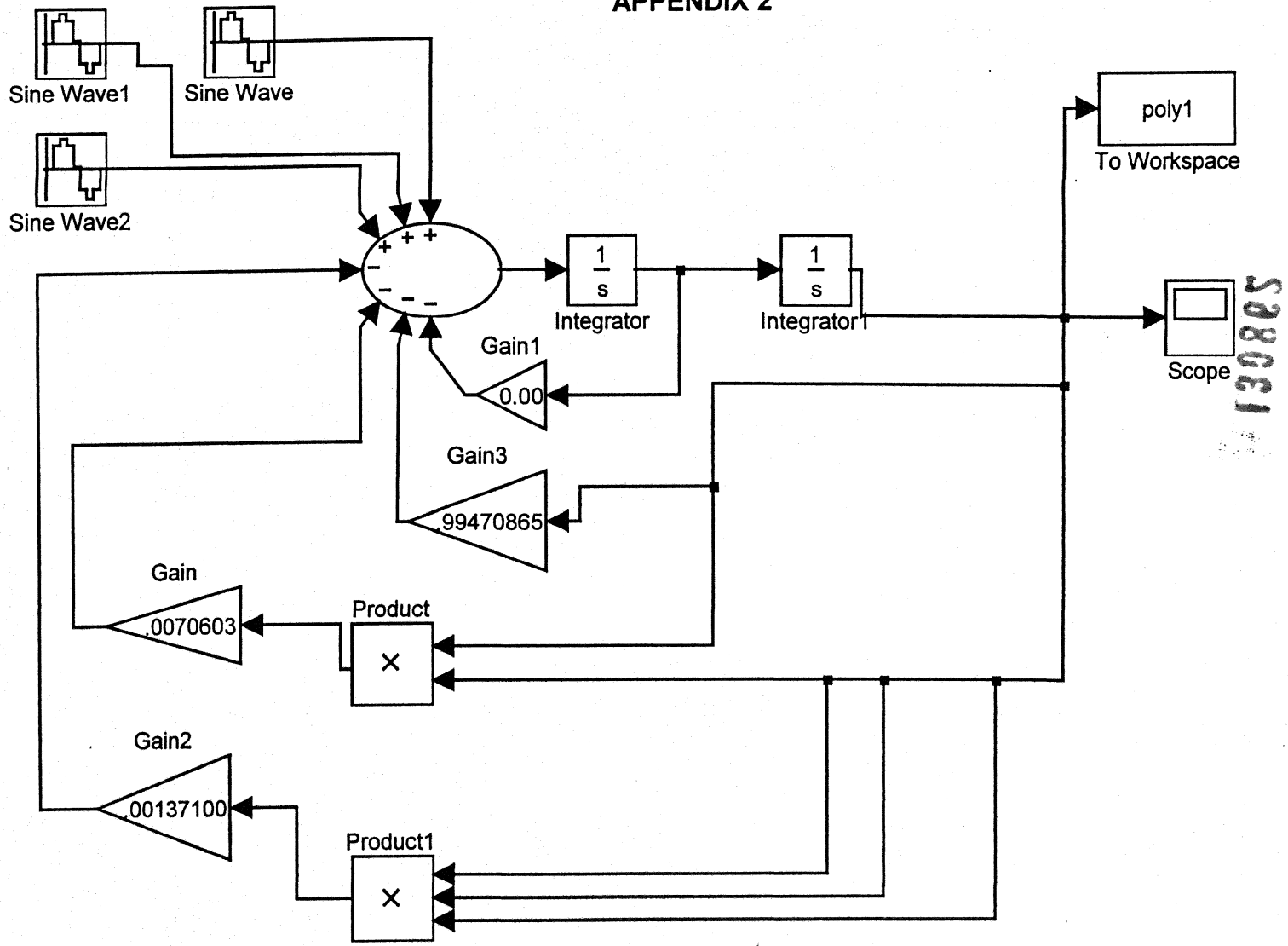

SIMULINK MODEL FOR EQUIVALENT POLYNOMIAL MODEL RESPONSE